Spectroscopic Analysis of Radiation-Generated Changes in Tensile Properties of a Polyetherimide Film

Edward R. Long, Jr.,
and Sheila Ann T. Long

--   1   OF   1
                        DTIC DOES NOT HAVE THIS ITEM
--
-- 1 -   AD NUMBER: D439442
-- 5 -   CORPORATE AUTHOR: NATIONAL AERONAUTICS AND SPACE ADMINISTRATION
--   HAMPTON VA LANGLEY RESEARCH CENTER
-- 6 -   UNCLASSIFIED TITLE: SPECTROSCOPIC ANALYSIS OF RADIATION-
--   GENERATED CHANGES IN TENSILE PROPERTIES OF A POLYETHERIMIDE FILM,
--10 -   PERSONAL AUTHORS: LONG,E. R. , JR.;LONG,S. A. ;
--11 -   REPORT DATE: MAY   , 1985
--12 -   PAGINATION: 36P
--14 -   REPORT NUMBER: NASA-TP-2429, L-15873
--20 -   REPORT CLASSIFICATION: UNCLASSIFIED
--22 -   LIMITATIONS (ALPHA):   APPROVED FOR PUBLIC RELEASE; DISTRIBUTION
--   UNLIMITED. AVAILABILITY: NATIONAL TECHNICAL INFORMATION SERVICE,
--   SPRINGFIELD, VA. 22161. NASA-TP-2429.
--33 -   LIMITATION CODES: 1

-- END   Y FOR NEXT ACCESSION   END

Spectroscopic Analysis of Radiation-Generated Changes in Tensile Properties of a Polyetherimide Film

Edward R. Long, Jr.,
and Sheila Ann T. Long

Langley Research Center
Hampton, Virginia

SUMMARY

The effects of electron radiation on Ultem, a polyetherimide manufactured by General Electric, were studied for doses from 2×10^9 to 6×10^9 rad. Specimens for tensile property testing and for electron paramagnetic resonance (EPR) and infrared (IR) spectroscopic measurements of molecular structure were studied. The spectroscopic data were used to determine the effects of radiation on molecular structures, and these effects were used to explain the radiation-generated changes in tensile properties.

Because the cross-sectional area of the electron beam was limited to a 6-inch diameter, miniature tensile specimens were used. Extensive testing was conducted to develop the size and test procedure for the tensile specimens. The miniaturization was based upon ASTM Testing Standard 882. A design for a Faraday cup and the use of a remote IR temperature sensor are also described. The Faraday cup was used to monitor the electron beam current; it was calibrated with NBS-traceable nylon films, which were used to measure the total dose. The IR temperature sensor was used to remotely monitor the specimen temperature during exposure.

The spectroscopic data showed that radiation caused dehydrogenation of the pendent methyl groups, rupture of the main-chain bonds at the ether linkage sites, and opening of imide rings, all to form radicals. The spectroscopic data also indicated that the so-formed atomic hydrogen attached to phenyl radicals, but not to phenoxyl radicals, which would have formed hydroxyls. Therefore, the observed decays of the radiation-generated phenoxyl, gem-dimethyl, and carbonyl radicals were interpreted as a combining of the radicals to form crosslinking. This crosslinking is the probable cause of the major reduction in the elongation of the tensile specimens after irradiation. The tensile testing showed a 22-percent decrease in tensile strength, a 96-percent decrease in strain to failure, and an 8- to 10-percent increase in modulus for the 6×10^9 rad dose. Subsequent classical solubility tests indicated that the irradiation did cause massive crosslinking.

INTRODUCTION

For approximately two decades aerospace scientists in materials research have recognized the advantages of using fiber-reinforced resin composites (FRRC) for space structural components. The principal advantages are high specific strength, stiffness, and low thermal expansion. Moreover, the specific values for these properties are easily tailored. However, the long-term stability of these materials when subjected to electron, proton, and ultraviolet radiations must be established. For large space structures that have mission lives up to 30 years, in orbit about Earth in radiation belts, radiation durability is an important consideration.

The literature contains much information about the space application of polymeric materials and the effects that space environmental parameters may have on material properties. Useful, though not fully current, information is available in a materials handbook for space (ref. 1). The handbook includes data and models for the amounts of radiation in orbital environments about Earth, descriptions for classes of materials (thermal control, optical, adhesives, structural, and electronic), descriptions of the effects of environmental parameters on materials, data

from space applications of materials, and guidelines for the selection of materials. Reference 2 provides an additional description of Earth-orbital environments, reference 3 describes low Earth-orbital environments, and reference 4 provides environmental data for geosynchronous orbit. The models for these descriptions are continually updated. Also, reports have been published which review and summarize research regarding radiation effects on materials. An example is reference 5; it contains information from a NASA meeting on space radiation damage and on proposed additional research within the agency. References 6-9 are also summary reports which address the environmental effects issue and indicate that interest in radiation effects is increasing within a very broad research community.

Several textbooks (refs. 10-15) discuss radiation effects at a generic level. The data are for relatively simple molecular systems and make a valuable contribution toward a general understanding of radiation effects.

The number of reports of studies of radiation effects on specific materials is very large, so only a few relevant ones will be discussed. Reference 16 is an example of a study of radiation effects on polymeric systems. The data show that the net effects of radiation are crosslinking and bond scission. However, the effect which dominates varies with the polymer system in question. For simple chemical structures, polymers may be grouped according to the net effect. This report also evaluated the radiation resistance of two more complicated polymer systems, epoxy and polyimide. Although the quantitative meaning of the expression "radiation resistance" is not defined in the report, the epoxy and the polyimide generic classes were suggested as more suitable for a radiation environment than the other polymers studied.

The study of radiation effects on polyimides has centered on Kapton manufactured by E. I. du Pont de Nemours & Co., which is available in film form. Reference 17 reported a study of the tensile properties for radiation doses up to 2×10^9 rad. The changes were found to be insignificant. A more recent investigation of the same material (refs. 18 and 19) also showed that the tensile properties did not significantly change. Using IR spectroscopy, this study determined that the effects on the chemical structure, which occurred at the carbonyl sites and at the ether-linkage sites, were small. Any changes that may have occurred resulted primarily from thermal effects because of the high dose rate.

During the early to mid 1960's, a series of radiation-effects studies were made for polymeric structures (refs. 20-28). These reports showed that if radiation doses were applied too quickly, they caused thermal effects that could be misinterpreted as simply radiation effects. The studies also found that radiation durability of polymer materials could be improved by using more complicated structures. The limitation of this solution for the radiation problem was that sufficiently radiation-durable polymers were intractable to processing. An example of this limitation was pyrrone (short for polyimidazopyrrolone), a ladder polymer which was essentially radiation resistant.

These and other data provide a basis for a general understanding of radiation effects. However, for new, complex polymer systems, many of the questions dealing with radiation durability will have to be readdressed. There are several reasons why. First, energy absorbed at one site in a molecular structure is frequently transferred to another. The absorption site, the site to which transfer occurs, and the final effect depend not only on the polymer's individual components of molecular structure but also on how the components are tied together. Consequently, simpler molecular systems, whose structures are a part of the complex ones, do not model the

complex system's response to radiation. Similarly, the response of one complex system is not necessarily that of another, because of the differences in their molecular structure.

Another reason for continuing radiation-effects studies is the concern for whether or not laboratory simulations of exposure to space environmental parameters are sufficiently correct. An example of this is dose rate. Some of the research reported in references 20-28 indicated that thermal effects could be avoided if a dose rate of 3×10^9 rad/hour was not exceeded. It was assumed that if the dose rate did not cause an increase in temperature up to the polymer's glass transition temperature, then the thermal effects were not important. While that may be true, the assumption would appear to be undergoing reconsideration.

This paper reports a study of a polyimide which possesses thermoplastic properties. The material is Ultem, a polyetherimide. Ultem is one of the many newly available, toughened polymers. Because it is a thermoplastic, Ultem can be used in film, casting, and FRRC forms. Thus it may be both radiation durable and processable.

Total radiation doses from 2×10^9 to 6×10^9 rad were investigated because these are representative of the dose expected for a 10- to 30-year mission in geosynchronous orbit. The specimen temperature during exposure and the time interval between exposure and testing were important considerations. The polymer was studied in film form in order to compare infrared and electron paramagnetic resonance spectroscopy data with tensile mechanical data.

EXPERIMENTAL

Electron Gun

The source of electron radiation was an RCA model EMU3-H transmission electron microscope. The microscope was operated at 100 keV. The objective lens was removed in order to obtain a higher than normal beam current at the fluorescent surface of the viewing area. The beam was approximately 6 inches in diameter at the viewing surface. The beam uniformity was determined to be within 5 percent by using an array of collectors placed upon the viewing surface. The specimens were mounted on holders and placed in the viewing area for exposure. The front window of the viewing area was modified for easy access to the specimens within 1 minute after the end of an exposure.

Faraday Cup and Thermal Sensor

The standard RCA fluorescent surface in the viewing area was replaced with a ZnS-coated plate which held a Faraday cup at the center position of the electron beam. The ZnS was covered with a 0.2-mil-thick film which prevented contamination of specimens during exposure but which was thin enough for electron penetration and luminescence of the ZnS. A cross-sectional view of the cup and a portion of the ZnS-coated plate is shown in figure 1. The collector was graphite and was shaped to minimize backscatter. The entrance hole diameter was 1/8 inch and the collector's interior length was 1 inch. The collector was shielded by an aluminum jacket; the insulation between the jacket and cup was Teflon manufactured by E. I. du Pont de Nemours & Co. The Faraday cup current was monitored with a model 425A DC micro

volt-ammeter manufactured by Hewlett Packard Company. The cable from the cup to the meter was triple-shielded and routed to prevent spurious inputs.

The temperature sensor was a model 12-521 infrared research thermometer manu-factured by Barnes Engineering Company. The thermometer monitored the specimen's IR emission at 8 to 13 micrometers through a sodium chloride single crystal which was inserted into one of the viewing area's side windows.

Mechanical Tester

A model 1130 table-top Instron mechanical testing instrument was used for measuring tensile properties. Pneumatically actuated grips with hard rubber-surfaced, steel faces were used. A direct-current displacement transducer (DCDT) was attached to the grips to record their separation. The DCDT output was used as an input to the X-axis of a recorder, while the load cell signal was the input for the recorder's Y-axis. All mechanical property measurements were made at room temperature.

Infrared Spectrometer

The IR spectra were recorded from 4000 to 200 cm^{-1} with a model 599B Perkin-Elmer spectrometer. The spectrometer was a grating type with a 1-cm^{-1} resolution. The scan time was 6 minutes. The spectrometer was controlled by a model 3500 Perkin-Elmer data station. Spectra were recorded and stored for each specimen immediately before and after exposure. For each recording, the spectrum of a poly-styrene standard was also recorded and stored to provide a basis for normalizing the effects that any day-to-day variation in recording had on spectra magnitudes. The specimens' IR spectra were recorded at room temperature.

Electron Paramagnetic Resonance Spectrometer

A Varian E-line Century Series EPR spectrometer (model/part no. 90679007 AL) was used to measure the unpaired electron (radical) sites caused by the irradiation. A precision frequency meter was used to monitor the frequency of the microwave source. A variable temperature accessory was used to maintain the specimen temper-ature at -188°C during a measurement.

Specimens

Fabrication.- The specimens were fabricated from Ultem film. The molecular structure of Ultem is shown in figure 2. The tensile and EPR specimens were approx-imately 0.003 inch thick. The IR specimens were approximately 0.0003 inch thick.

The tensile and EPR specimens were fabricated in two steps. First, strips were cut to the respective dimensions of the two different specimen widths by using the fixture shown in figure 3. The fixture consisted of a 1.0-inch-thick glass plate to which was attached a Teflon-coated steel guide bar. A truck mounted on the guide bar was hand propelled to cut a strip in a single stroke. The cuts were made by two standard single-edge razor blades whose stiff backs had been removed to facilitate holding the blades flush with the spacer between them. The dimensions of the spacers were machined to provide the widths of the respective specimens. Second,

the specimens were cut to length from the strips. The lengths of the EPR specimens were critical; therefore, a second fixture, shown in figure 4, was used to cut them to exact length with their ends perpendicular to their sides. The cutting bar for this fixture consisted of two single-edge razor blades (stiff backs removed) whose edges were separated by the bar by an amount equal to the EPR specimen length. The cutting bar was lowered between the Teflon-coated guide blocks to the glass surface, where the strip of film was held perpendicular to the blades by an alignment bar. The cutting bar was then pressed upon the strip, and the blades cut away a specimen of very precise length. Since the lengths of the mechanical specimens and the direction of their ends were not critical, the mechanical specimens were cut from their strips with scissors. The edges of each specimen were inspected with an optical comparator and discarded if any imperfections were found.

The IR specimens were fabricated from approximately 0.0003-inch film so that transmission IR spectroscopy could be performed. The dimensions of the IR specimens were not critical, except that the specimens needed to be sufficiently large to cover the spectrometer entrance slit.

Tensile.- The tensile specimens were 0.2 ± 0.001 inch wide and 6.0 ± 0.25 inch long. Each specimen thickness was determined to within 0.00005 inch with a Starrett no. 673 bench-top comparator. This is a smaller specimen for tensile properties of film than recommended by ASTM standard D 882 (ref. 29), but its dimensions are based upon that standard. The smaller size was required because the exposure area, as explained above, was limited to a 6-inch diameter. The 0.2-inch width was chosen because reference 29 suggests widths from 0.2 to 1.0 inch. For a 0.2-inch width, the minimum requirement of a width-to-thickness ratio of 8 is exceeded. Since reference 29 also requires the ratio of gauge length (distance between grips) to width to be at least 10, a gauge length of 2.0 inches was chosen. An additional length of 1.5 inches was required for each grip and another 1 inch was included for handling the specimen during alignment in the grips. Hence, the length of a specimen was 6 inches.

Six specimens were used per exposure. They were tested for elastic modulus properties at a crosshead speed of 0.02 inch per minute; the speed was determined from the initial strain rate suggested by reference 29. This crosshead speed was also used for testing their ultimate stress. For nonirradiated specimens, a crosshead speed of 0.10 inch per minute was used for the ultimate-stress portion of the test.

Each group of six specimens was held on a rectangular metal frame by polyimide tape for an exposure as shown in figure 5. Within 3.5 minutes after completion of an exposure the six specimens were immersed and kept in liquid nitrogen until just prior to each specimen's testing. The specimens were then brought, one at a time, to room temperature in a dry environment, installed in the grips, and tested at room temperature. (Separate tests determined that the temporary storage in liquid nitrogen had no effect on the film's nonirradiated tensile properties.)

Other separate tests on nonirradiated specimens were conducted to determine what differences there were for tensile properties for small (0.2 inch by 6.0 inch, 2.0-inch gauge) and full-size (1.0 inch by 14 inch, 10.0-inch gauge) film specimens. Table I contains the results for two materials, Kapton (a polyimide) and Union Carbide P1700 (a polysulphone). For each material, 50 small and 20 full-size specimens were tested. A comparison of the data clearly indicates that for measurements of changes in tensile properties of films the data for small specimens are acceptable.

Before any radiation exposures were conducted, approximately 200 small specimens of Ultem were tested to establish a data base. The data from these tests are given in table II, which also contains data obtained from the manufacturer of Ultem. The manufacturer used dog-bone shaped, molded specimens and testing procedures as recommended by ASTM D 638 (ref. 30). Even though different ASTM standards were used, making the specimen shape and procedures different, the two sets of data compare well for modulus and ultimate stress, while the elongation data agree within a factor of 2.

Electron paramagnetic resonance.- The EPR specimens were 0.100 ± 0.001 inch wide and 0.600 ± 0.003 inch long. Each specimen thickness was measured to within 0.00005 inch. Precision and repeatability were required for specimen dimensions in order to interpret the EPR signal in units of spins per cubic centimeter. (After all measurements were completed, the specimens were also weighed on a semimicro-balance to determine the EPR signal in terms of spins per gram and to check the spins per cubic centimeter using the polymer density.)

During an exposure, the EPR specimens were held on a metal strip by lengths of bent wire, as shown in figure 6. This method of holding minimized the amount of shadowing caused by the holder. The specimens could not be held with adhesives, tapes, etc., without introducing foreign substances into the EPR measurement.

Within 3.5 minutes following the end of an exposure, four specimens were inserted into each of four quartz glass EPR tubes. The tubes were temporarily sealed with silicon rubber caps and nylon clamps and immersed in a liquid nitrogen bath. When the specimens were to be maintained under vacuum, the tubes were partially raised out of the liquid nitrogen and a vacuum pulled with a turbo molecular pump. When a vacuum of approximately 10^{-8} torr was reached, the tube was sealed with a propane torch to form an ampule. The specimens remained in the bottom of the tube at liquid nitrogen temperature throughout this procedure.

The specimens were kept in the liquid nitrogen bath until EPR data were to be recorded. A tube of specimens was then immediately transferred to the EPR spectrometer's resonance cavity where the temperature was maintained at -188°C, the lower limit of a Varian EPR variable temperature accessory. At the end of an EPR scan the tube was returned to the liquid nitrogen bath. When radical decay data were desired, the tube was next brought to 22°C or 125°C (depending on the decay temperature studied) for the desired time interval; then additional EPR data were taken at -188°C. This cycle of liquid nitrogen storage, decay, and EPR scanning was repeated until the collection of decay data was completed.

Infrared.- There was one IR specimen per exposure. Specimens were mounted with polyimide tape on a rectangular, thin-metal frame which was the size of the specimen. Specimens were scanned at room temperature beginning approximately 5 minutes after the completion of exposure.

RESULTS AND DISCUSSION

Dose and Temperature Measurements

Prior to exposures, the radiation doses and specimen temperatures were established as a function of Faraday cup current. Both variables can be difficult to measure; unforeseen parameters can affect the measurement results. Consequently, considerable time was given to understanding the measurement results.

Dose measurements.- The doses corresponding to Faraday cup currents were determined with NBS-traceable nylon film whose optical density varies in known amounts with radiation dose. Figure 7 is a plot of the nylon's actual absorbed dose, as determined from densitometer readings, for a number of Faraday cup currents. The exposure time was 1 minute. Calculations of the absorbed dose were made using the Bethe-Block stopping power expressions (refs. 31-33) for several Faraday cup currents. These expressions can be used for a wide assortment of target materials (refs. 34 and 35). The calculations took backscatter into consideration, as prescribed by S. M. Selzer (an author of ref. 34) in personal communication. The backscatter was caused by the surface which supported the nylon in the target area. The dose predicted by the calculation agreed within 10 percent with the dose indicated by the nylon film.

The dose indicated by the nylon film was then corrected for the differences in density and stopping power between nylon and Ultem, in order to determine the radiation dose for Ultem in terms of Faraday cup current.

Temperature measurements.- Infrared remote sensing, instead of thermocouples, was selected for measuring specimen temperature during irradiation. The arrangement for measurements is shown in figure 8. Before making the measurements of specimen temperature in a radiation environment, the infrared sensor's measurements were calibrated against those of a calibrated thermocouple. A film specimen on an electrically heated surface was temporarily placed in the exposure chamber. The IR sensor was located and oriented to view the same spot on the specimen surface adjacent to the Faraday cup's entrance hole as it would, later, during radiation exposure. A thermocouple bead was placed on the specimen adjacent to the spot being viewed by the IR sensor. The IR sensor readings were then calibrated against those of the thermocouple while the chamber was under vacuum. A single-crystal sodium chloride window was used for the viewing port of the IR sensor. The effects of aging of the sodium chloride window were monitored.

Finally, prior to monitoring the temperature of the film as a function of dose rate (Faraday cup current), calculations using the Stephan-Boltzmann equation were made to determine the temperature rise during various dose rates due to radiative transfer. Since the equation does not include a conductive term, it is a highest temperature analysis and was not intended for accuracy. During the first portion of an exposure with the specimen supporter by the Ultem O-ring (fig. 8), there was no radiative conduction. The temperature increase measured at the beginning of an exposure did appear to be in agreement with predicted values from the Stephan-Boltzmann equation. For long exposures, several hours, the temperatures became higher as the general environment within the exposure chamber absorbed the radiation energy and came to equilibrium.

Figure 9 shows the equilibrium specimen temperatures at various cup currents for two methods of specimen support. The copper plate (coated with zinc sulfide) was the arrangement used for specimen support for the property data to be discussed.

A temperature of 38°C (100°F) was selected as the maximum elevated temperature to be allowed during an exposure. This temperature was not quite reached for a Faraday cup current of 20 nanoamperes. For Ultem, this current corresponds to an upper limit for the dose rate of 10^9 rad per hour.

Whether or not setting a low temperature limit is an adequate criterion for accelerated exposures is not certain. The work reported in references 20-28 limited the dose rate to approximately 3×10^9 rad per hour. From figure 9, this dose rate

would cause a temperature of approximately 70°C (155°F). Obviously, the temperature criteria are more stringent for the work in this report.

Radiation Exposure Data

Electron paramagnetic resonance spectra.- EPR spectroscopy detects and measures the presence of unpaired electrons, which are called radicals. The EPR data were used to identify the radicals created by the radiation and to determine their concentrations and decay rates. Radicals are the intermediate products of electron radiation for polymers, and they are created by the homolytic cleavage of covalent molecular bonds. The radical density is a measure of the level of chemical activity created by the radiation and, therefore, should vary with dose rate, if the dose rate is sufficiently high. Figure 10 shows that the radical density at the end of a total exposure of 4.0×10^9 rad was the same for an 8-hour (5.0×10^8 rad per hour) and a 16-hour (2.5×10^8 rad per hour) exposure. Consequently, there was no dose-rate effect observed. (Also, no differences were observed in the infrared and mechanical data for these same two exposures.) Whether or not a saturation had occurred at these dose rates cannot be stated because lower dose rates were not used. However, comparison of these dose rates with those reported in references 36-39, 3.0×10^8 rad per hour for electron radiation and 2.25×10^5 rad per hour for gamma radiation, suggests that the radiation effects upon Ultem reported in this paper are probably the ones which would occur in the geosynchronous orbital environments. This is because the referenced work showed that the effects of the electron and gamma radiation were the same. The gamma radiation dose rate was only 10 to 100 times that in geosynchronous orbit. That probably was not high enough to cause an acceleration effect.

Figure 11 shows the post-exposure decay in air at 125°C and 22.5°C. The decay rate increased with temperature. (No decay occurred at the temperature of liquid nitrogen; consequently, it was chosen as the storage temperature.) Figure 12 shows that the decay was significantly faster in air than in vacuum. This was the reason for storing in vacuum.

Figure 13 shows a typical EPR spectrum for irradiated Ultem. This spectrum is representative for the doses studied, in that it consists of four individual parts as indicated in the figure. Each part was due to a different radical. Each part was a first-derivative curve of an absorption peak; however, the four overlapped as shown. The total radical density (sum of the four parts) varied with radiation dose as shown in figure 14; i.e., the radiation increased the radical (spin) density by over two orders of magnitude. These spin densities were recorded immediately after the completion of each exposure. The decay of the total spin density for all four radicals, at room temperature and under vacuum, is shown for a total dose of 6.0×10^9 rad in figure 15.

One important use of the EPR data is to identify the radicals formed by the radiation. The information extracted from the spectra - such as the total width of each part, the peak-to-peak widths, the electronic g-values, and the decay rates - contributes to the identification.

Figures 16 and 17 combine to demonstrate an example for using decay rates for spin labeling. Kapton is another polyimide, the structure of which, though very similar to that of Ultem, differs in that it does not have methyl pendent groups. In air (fig. 16), the radical decay was more rapid for Ultem than it was for Kapton.

In vacuum (fig. 17), the decay rate was the same for the two materials. The difference in air was that, for Ultem, the molecular oxygen from the air was first taken up by the gem-dimethyl radical to form a peroxide radical. The peroxide gem-dimethyl radicals decay faster (ref. 40) than the gem-dimethyl radicals. The EPR signals due to the peroxide gem-dimethyl (ref. 40) and the gem-dimethyl (ref. 41) are very characteristically different. The reference values for the g-values and line widths were used to assign part 2 of the EPR spectrum as due to the gem-dimethyl radical.

An additional ingredient for radical identification is the radical lifetime after the completion of exposure. Figures 18 and 19 demonstrate that the lifetime of each radical was different. From both figures, one observes that the magnitudes of the individual parts decayed and that the relative values of these magnitudes changed with time. These observations are substantiated by the fact that the g-value for the sum of the four parts changed with time. The change in the g-value is a guide to the amount the magnitudes of the four radical densities were changing with respect to each other.

Figures 18 and 19 show that the g-value for the sum of the four parts also changed with dose. This is shown more clearly in figures 20 and 21. The g-value consistently increased with dose and consistently decreased with time. Thus, irrespective of the initial spin densities and their distributions, the respective radicals each decayed in an individual manner.

The four parts of the EPR spectrum are identified in figure 13. Radical 1 is believed to be a phenoxyl (ref. 42); radical 2, as stated earlier, is a gem-dimethyl (refs. 40 and 41); radical 3 is a carbonyl (ref. 43); and radical 4 is a cyclohexadienyl (refs. 44 and 45). The total line widths for these four radicals are approximately 41, 94, 108, and 160 gauss, respectively. These four radicals are shown in figure 22, along with the phenyl radical and atomic hydrogen. Although the latter two were not observed, they had to have been formed during the exposure. These highly reactive radicals were not observed because their lifetimes were too short for them to have been seen (refs. 46-48). One reason for the short lifetimes is that the phenyl structure has a strong affinity for hydrogen (ref. 49).

Infrared spectra.- Infrared spectroscopy provided a fingerprinting for the material. The recording of a specimen's IR spectra before and after radiation exposure facilitated the measuring of changes in the absorption bands of the material, that is, changes in atom-atom bond populations caused by the radiation. The IR spectrum for nonirradiated Ultem is shown in figure 23. The bands in figure 23 are numbered; they are identified in table III. The bands were identified using references 50-52.

The changes which occurred upon exposure to the radiation doses are shown in figure 24 and listed in table IV. The spectra in figure 24 are differences of the absorption bands for the Ultem specimen before and after irradiation. A positive value represents an increase in the magnitude of the absorption band.

Comparison of EPR and IR spectra.- Only the changes due to 6×10^9 rad exposure are discussed. The IR C-H methyl band at 2960 cm^{-1} decreased because of dehydrogenation of the methyl pendent group. This is substantiated by the occurrence of the EPR spectra for a gem-dimethyl radical. As noted in the discussion of the EPR spectra, an atomic hydrogen radical also had to be formed, even though it was not observed. The hydrogen radical was not seen because it is highly reactive; it either forms molecular hydrogen or attaches to a phenyl site. Molecular hydrogen is a

typical outgassing product. The attachment to a phenyl site was substantiated by the EPR data showing the formation of cyclohexadienyl radicals and by the IR data showing increases in the mono-substituted phenyl and in the C-H (phenyl) bands. The mono-substitution was interpreted as occurring at a phenyl radical site created by homolytic chain scissioning of the ether linkage at the para-substituted benzene ring. The phenyl radical combined with the hydrogen atom to form a mono-substituted phenyl structure. The formation of the cyclohexadienyl radicals was not surprising, since the benzene ring does trap atomic hydrogen. The EPR spectra included phenoxyl radicals (fig. 13) which were observed to decay (figs. 18 and 19). Chemically, one very likely mode for this decay would be to form hydroxyl end groups; however, no hydroxyl formation was observed in the IR spectra. (Of course, the hydroxyl formation may be hard to see in the IR spectra.) Therefore, the phenoxyl radicals most likely formed crosslinking bridges upon their decay.

The formation of phenoxyl radicals and a decrease in the IR absorption band for ether (aromatic) were definite indications of chain scissioning at the ether linkage. Which side of the ether linkage was severed is not clear. The IR bands at 775 cm^{-1} and 845 cm^{-1} represent both para- and tri-substituted phenyl structures. A decrease in the tri-substitution results in an increase in the ortho-substitution, while a decrease in the para-substitution produces mono-substitution. There was an indication of a mono-substituted product because of the small increase in the band at 680 cm^{-1}. On the other hand, since the bands for ortho-substitution overlap those for para- and tri-substitution, any increase in ortho-substitution would not be detected.

The 6 x 10^9 rad dose also caused a significant amount of opening of the imide ring as interpreted from the decreases in the absorption bands at 1780, 1720, 1355, and 740 cm^{-1}. Indeed, this would appear to have been the case because the EPR spectra showed a carbonyl radical. The carbonyl radicals were probably formed by bond breakage between the carbonyl carbon and the phenyl carbon. This is suggested by a lack of change in the C-N band. The formation of both para- and meta-substituted phenyl structures can occur when the imide ring is opened in this manner; both products further complicate the interpretation of changes in the magnitudes of the substituted-phenyl bands.

The molecular structural changes which occurred are summarized in figure 25. The top line shows the two possibilities for scission at the ether linkage, along with dehydrogenation of the methyl group and mutual cancellation of the phenyl and atomic hydrogen radicals. The center line shows the formation of the cyclohexadienyl radical, which can accompany dehydrogenation when the ether linkage remains intact. The bottom line shows the carbonyl radical formed when the imide ring is opened. There are two possible openings, both of which are accompanied by hydrogen attachment to the phenyl radical. As one sees from figure 25, given the lack of availability of hydrogen, the most likely mode of decay for the carbonyl, gem-dimethyl, and phenoxyl radicals was crosslinking, because hydrogen attachment at phenyl sites prevented recombination, and because there was no evidence of hydroxyl end-capping.

The interpretation of changes in tensile properties.- The changes in the average tensile properties of the Ultem film are shown in figures 26-28. Table V lists additional data for these changes. The radiation reduced the tensile strength; the maximum change was 22 percent for 4 x 10^9 rad. The modulus changes were less than 10 percent. The changes in elongation were larger. A 96-percent decrease occurred for 6 x 10^9 rad. This suggests that significant embrittlement occurred. Since the strength did not increase (indeed, it decreased), this embrittlement may also be

10

interpreted as a decrease in material toughness. Figure 29 is a drawing of the elongations which occurred. For nonirradiated specimens the failure was preceded by a localization of sample necking.

Most of the elongation for nonirradiated Ultem is a plastic deformation. Therefore, it is reasonable to assume that the reduction in elongation of the irradiated specimens was due to a radiation-induced mechanism which reduced the slippage of the adjacent linear molecules relative to one another. This is exactly what is shown by the IR and EPR data. These spectroscopic data showed main-chain breakage at ether linkages and dehydrogenation of the methyl pendent groups. The IR data showed no formation of hydroxyls, and the EPR data showed no oxygen radicals and no phenyl radicals. Thus, the radicals most likely combined to form aliphatic-, carbonyl-, and oxygen-bridging cross linkages between molecules. Indeed, subsequent solubility tests on the irradiated and nonirradiated material, using chloroform and tetrachloroethane, showed that the radiation caused massive crosslinking.[1] This crosslinking was the cause of embrittlement. Some of the oxygen bridges were most likely peroxide structures. Since the oxygen-oxygen bond is several times weaker than the oxygen-carbon bond, which was severed at two sites in order to form the peroxide linkage, the resulting molecular structure is weaker. This weaker structure would contribute, in part, to the decrease in tensile strength.

A potential contribution to the smaller decrease in tensile strength at the highest dose can be argued on the basis of the observations from the IR and EPR data that the imide ring was opened at higher doses. The crosslinking formed by the dangling side of the carbonyl structure would lead to ladder crosslinking, which is both strong and rigid. Hence, the net effect of both the peroxide and the ladder crosslinking would be less change in the tensile strength.

Another effect of the ladder structure would be an increase in the modulus. This is because the ladder crosslinking would increase the load required for an elastic deformation. Indeed, there is an increase in modulus, although a small one, at the 6×10^9 rad dose.

Perhaps the most significant observation to be made from the mechanical data is that considerable embrittlement occurred along with a decrease in ultimate strength. This results in a less tough resin.

CONCLUDING REMARKS

The effects of 100-keV electron radiation on Ultem, a polyetherimide, were studied for doses from 2×10^9 to 6×10^9 rad. Specimens for tensile property testing and for electron paramagnetic resonance and infrared spectroscopic measurements of molecular structure were studied. The spectroscopic data were used to determine the effects of radiation on molecular structure, and these effects were used to understand the radiation-generated changes in tensile properties.

The tensile data showed extensive embrittlement due to the crosslinking. Some decrease in strength also occurred, perhaps because the crosslinking consisted

---

[1]The authors wish to thank Dr. Vernon L. Bell, Langley Research Center, for suggesting the solubility tests and for providing time and facilities to perform them.

of bonds, such as peroxides, that were weaker than the original ones broken by the radiation. The embrittlement and decreased strength caused a radiation product which is less tough than the original material.

The spectroscopic data showed that radiation caused dehydrogenation of methyl groups, rupture of main-chain ether linkage, and opening of imide rings, all to form radicals. The spectroscopic data also indicated that the so-formed atomic hydrogen attached to phenyl radicals, but not to phenoxyl radicals which would have formed hydroxyls. Therefore, the observed decays of the radiation-generated phenoxyl, gem-dimethyl, and carbonyl radicals were interpreted as a combining of the radicals to form crosslinking. This crosslinking is the probable cause of the major reduction in the elongation of the irradiated tensile specimens. The tensile testing showed a 22-percent decrease in tensile strength, a 96-percent decrease in strain to failure, and an 8- to 10-percent increase in modulus for the 6×10^9 rad dose. Subsequent classical solubility tests indicated that the irradiation did cause massive crosslinking.

NASA Langley Research Center
Hampton, VA 23665
January 31, 1985

12

REFERENCES

1. Rittenhouse, John B.; and Singletary, John B.: Space Materials Handbook, Third ed. NASA SP-3051, 1969. (Available as AMFL-TR-68-205.)

2. West, G. S., Jr.; Wright, J. J.; and Euler, H. C., eds.: Space and Planetary Environment Criteria Guidelines for Use in Space Vehicle Development, 1977 Revision. NASA TM-78119, 1977.

3. Watts, John W., Jr.; and Wright, Jerry J.: Charged Particle Radiation Environment for the Spacelab and Other Missions in Low Earth Orbit - Revision A. NASA TM X-73358, 1976. (Supersedes NASA TM X-64936.)

4. Wright, J. J.; and Fishman, G. J.: Radiation Environment and Hazards for a Geosynchronous Space Station. NASA TM X-64983, 1976.

5. Proceedings of Meeting on Charged Particle Radiation Effects. NASA TM-82259, 1964.

6. Materials for Space Operations. NASA SP-27, 1962.

7. Materials in Nuclear Applications. ASTM Spec. Tech. Publ. No. 276, 1960.

8. Environmental Effects on Advanced Composite Materials. ASTM Spec. Tech. Publ. 602, c.1976.

9. van der Waal, P. C.: Effect of Space Environment on Materials, First ed. Rep. No. RV-22, Royal Netherlands Aircraft Factories Fokker (Schiphol-Zuid, The Netherlands), July 4, 1968.

10. Metz, D. J.: Testing Polymers for Radiation Resistance. Testing of Polymers, John V. Schmitz, ed., Volume 2, Interscience Pub., 1966, pp. 151-200.

11. Swallow, A. J.: Radiation Chemistry - An Introduction. John Wiley & Sons, Inc., c.1973.

12. Bolt, Robert O.; and Carroll, James G., eds.: Radiation Effects on Organic Materials. Academic Press, Inc., 1963.

13. Makhlis, P. A. (Israel Program for Scientific Translations, transl.): Radiation Physics and Chemistry of Polymers. John Wiley & Sons, [1975].

14. Chapiro, Adolphe: Radiation Chemistry of Polymeric Systems. Interscience Pub., 1962.

15. Charlesby, Arthur: Atomic Radiation and Polymers. Pergamon Press, Inc., 1960.

16. Van de Voorde, Marcel: Radiation Effects on Polymers. AEC-TR-6920, U.S. Atomic Energy Commission, [1967].

17. Price, Howard L.: Effect of Gamma Radiation in Vacuum on the Tensile Properties of Polymer Films. Paper presented at ASME 1967 Winter Annual Meeting (Pittsburgh, PA), Nov. 1967. (Available as NASA TM X-60858.)

18. Ferl, James E.; and Long, Edward R., Jr.: Low-Energy Electron Effects on Tensile Modulus and Infrared Transmission Properties of a Polypyromellitimide Film. NASA TM-81977, 1981.

19. Ferl, James E.; and Long, Edward R., Jr.: Infrared Spectroscopic Analysis of the Effects of Simulated Space Radiation on a Polyimide. IEEE Trans. Nucl. Sci., vol. NS-28, no. 6, Dec. 1981, pp. 4119-4124.

20. Bell, Vernon L.; and Jewell, Robert A.: Properties of Polyimidazopyrrolones. Paper presented at American Chemical Society Spring National Symposium on Ladder and Spiro Polymers (Miami, FL), Apr. 1967. (Available as NASA TM X-59873.)

21. Price, Howard L.; and Bell, Vernon L.: Radiation Stability of Unfilled Pyrrone Moldings. Materials and Processes for the 70's, Volume 15 of National SAMPE Symposium and Exhibition, Soc. Advance. Mater. & Process Eng., 1969, pp. 335-346.

22. Pezdirtz, George F.; Price, Howard L.; and Bell, Vernon L.: Radiation Effects on Aromatic Main Chain Polymers. Proceedings of Meeting on Charged Particle Radiation Effects, NASA TM-82259, 1964, pp. 103-125.

23. Bell, Vernon L.; and Pezdirtz, George F.: Poly(imidizopyrrolones): A New Class of Radiation Resistant Polymers. Paper presented at 150th National Meeting of American Chemical Society (Atlantic City, NJ), Sept. 1965. (Available as NASA TM X-57034.)

24. Bell, Vernon L.; and Pezdirtz, George F.: Polyimidazopyrrolones: A New Route to Ladder Polymers. J. Polym. Sci., Pt. B, vol. 3, no. 12, Dec. 1965, pp. 977-984.

25. Burow, S. D.; Pezdirtz, G. F.; Sands, G. D.; and Turner, D. T.: Degradation of Polyethylene Terephthalate by Gamma-Radiation. NASA TM X-61286, 1964.

26. Sands, George D.; and Pezdirtz, George F.: Cross-Linking of Polyvinylidene Fluoride by Gamma Radiation. Paper presented at the 150th National Meeting of American Chemical Society (Atlantic City, NJ), Sept. 1965. (Available as NASA TM X-57037.)

27. D'Alelio, G. F.; Haberli, Roland; and Pezdirtz, George F.: Effect of Ionizing Radiation on a Series of Saturated Polyesters. NASA SP-58, 1964.

28. Rogowski, R. S.; and Pezdirtz, G. F.: Electron Spin Resonance of γ-Irradiated Poly(ethylene 2,6-Naphthalene Dicarboxylate). J. Polym. Sci.: Pt. A-2, vol. 9, no. 12, 1971, pp. 2111-2117.

29. Standard Test Methods for Tensile Properties of Thin Plastic Sheeting. ASTM Designation: D 882-81. Part 35 of 1982 Book of ASTM Standards, c.1982, pp. 408-417.

30. Standard Test Methods for Tensile Properties of Plastics. ASTM Designation: D 638-82. Part 35 of 1982 Book of ASTM Standards, c.1982, pp. 233-249.

31. Bethe, H.: Quantenmechanik der Ein- und Zwei- Elektronenprobleme. Handb. Phys., Bd. XXIV, Kap. 3, Julius Springer (Berlin), 1933, pp. 273-560.

32. Bethe, H.: Zur Theorie des Durchgangs schneller Korpuskularstrahlen durch Materie. Ann. Phys., 5 Folge, Bd. 5, 1930, pp. 325-400.

33. Bethe, Hans A.; and Ashkin, Julius: Passage of Radiations Through Matter. Experimental Nuclear Physics, Volume 1, E. Segrè, ed., John Wiley & Sons, Inc., c.1953, pp. 166-357.

34. Berger, M. J.; and Seltzer, S. M.: Stopping Powers and Ranges of Electrons and Positrons, 2nd ed. NBSIR 82-2550-A, U.S. Dep. Commer., Feb. 1983. (Available from NTIS and PB83 175 687.)

35. Long, Edward R., Jr.: Electron and Proton Absorption Calculations for a Graphite/Epoxy Composite Model. NASA TP-1568, 1979.

36. Wolf, K. W.; Memory, J. D.; Gilbert, R. D.; and Fornes, R. E.: Effects of 0.5 MeV Electrons on the Interlaminar Shear and Flexural Strength Properties of Graphite Fiber Composites. J. Appl. Phys., vol. 54, no. 10, Oct. 1983, pp. 5558-5561.

37. Kent, George Michael: X-Ray and ESR Characterization of the Effects of High Energy Radiation of Graphite Fiber Reinforced Composite Materials. M.S. Thesis, North Carolina State Univ., 1982.

38. Fornes, R. E.; Memory, J. D.; and Naranong, N.: Effect of 1.33 MeV γ Radiation and 0.5 MeV Electrons on the Mechanical Properties of Graphite Fiber Composite. J. Appl. Polym. Sci., vol. 26, no. 6, 1981, pp. 2061-2066.

39. Kent, G. M.; Memory, J. M.; Gilbert, R. D.; and Fornes, R. E.: Variation in Radical Decay Rates in Epoxy as a Function of Crosslink Density. J. Appl. Polym. Sci., vol. 28, no. 10, 1983, pp. 3301-3307.

40. Pshezhetskii, S. Ya.; Kotov, A. G.; Milinchuk, V. K.; Roginskii, V. A.; and Tupikov, V. I. (P. Shelnitz, transl.): EPR of Free Radicals in Radiation Chemistry. John Wiley & Sons, Inc., c.1974.

41. Miyagawa, Ichiro; and Gordy, Walter: Deuterium Substitution in an Electron Spin Resonance Study of Radiation-Induced Free Radicals. J. American Chem. Soc., vol. 83, no. 5, Mar. 5, 1961, pp. 1036-1040.

42. Stegmann, H. B.; and Scheffler, K.: Sterisch ungehinderte Aroxyle. Z. Naturforsch, Teil B, vol. 19, no. 6, June 1964, pp. 537-538.

43. Smirnova, V. I.; Zhuravleva, G. S.; Yanova, K. G.; and Shigorin, D. N.: Electron Paramagnetic Resonance Study of the Structure and Behaviour of Radicals Generated Under the Action of Light and γ- and β-Radiation on Acetaldehyde and Formaldehyde. Russian J. Phys. Chem., vol. 38, no. 3, Mar. 1964, pp. 393-395.

44. Ohnishi, Shun-Ichi; Tanei, Tadayoshi; and Nitta, Isamu: ESR Study of Free Radicals Produced by Irradiation in Benzene and Its Derivatives. J. Chem. Phys., vol. 37, no. 10, Nov. 15, 1962, pp. 2402-2407.

45. Fessenden, Richard W.; and Schuler, Robert H.: ESR Spectrum of the Cyclohexadienyl Radical. J. Chem. Phys., vol. 38, no. 3, Feb. 1, 1963, pp. 773-774.

46. Tolkachev, V. A.; Chkheidze, I. I.; and Buben, N. Ya.: Electron Paramagnetic Resonance Spectra of Phenyl Radicals. J. Struct. Chem., vol. 3, nos. 1-6, 1962, pp. 682-684.

47. Long, S. A. T.; and Memory, J. D.: H-H, C-H, and C-C NMR Spin-Spin Coupling Constants Calculated by the FP-INDO Method for Aromatic Hydrocarbons. J. Magn. Reson., vol. 29, no. 1, 1978, pp. 119-124.

48. Wall, Leo A.; Brown, Daniel W.; and Florin, Roland E.: Atoms and Free Radicals by γ-Irradiation at 4.2°K. J. Phys. Chem., vol. 63, no. 10, Oct. 20, 1959, pp. 1762-1769.

49. Judeikis, Henry S.; Flournoy, John M.; and Siegel, Seymour: Isotope Effects and the Mechanism of Atom Production in Gamma-Irradiated Ice at 4.2°K. J. Chem. Phys., vol. 37, no. 10, Nov. 15, 1962, pp. 2272-2278.

50. Conley, Robert T.: Infrared Spectroscopy, Second ed. Allyn and Bacon, Inc., c.1972.

51. Cross, A. D.: An Introduction to Practical Infra-Red Spectroscopy. Butterworth & Co. (Pub.) Ltd., 1960.

52. Adrova, N. A.; Bessonov, M. I.; Laius, L. A.; and Rudakov, A. P. (Kurt Gingold, transl.): Polyimides - A New Class of Thermally Stable Polymers. Technomic Pub. Co., Inc., c.1970.

TABLE I.- TENSILE PROPERTIES FOR MINIATURE AND FULL-SIZE SPECIMENS USING ASTM TEST METHOD D882

Material	Modulus, 10^5 psi		Elongation, %		Ultimate stress, 10^4 psi	
	Miniature	Full size	Miniature	Full size	Miniature	Full size
Kapton	4.72 ± 0.13	4.89 ± 0.12	78 ± 5.0	65 ± 4.0	3.00 ± 0.02	2.70 ± 0.02
P1700	3.88 ± 0.31	3.89 ± 0.20	31 ± 4.0	59 ± 7.0	2.12 ± 0.01	1.78 ± 0.01

TABLE II.- TENSILE PROPERTIES FOR ULTEM FILM

Source (ASTM Standard)	Modulus, 10^5 psi	Elongation, %	Ultimate stress, 10^4 psi
Miniature (882)	4.27 ± 0.12	127 ± 0.07	1.72 ± 0.07
Manufacturer[a] (638)	4.30	60	1.52

[a]Manufacturer's data provided only average values.

TABLE III.- IDENTIFICATION OF THE INFRARED ABSORPTION BANDS OF ULTEM

Band number	Wave number, cm^{-1}	Bond	Reference
1	3060	C-H (phenyl)	50 (p. 116)
2	2960	C-H (methyl)	50 (p. 116)
3	1780	C=O pair (asymmetric)	50 (p. 155)
4	1720	C=O pair (symmetric)	50 (p. 155)
5	1600	C-C (phenyl)	51 (p. 52)
6	1500, 1480	C-C (phenyl)	51 (p. 52)
7	1445	$-CH_3$	50 (p. 99)
8	1355	$-CH_3$; C-N	50 (p. 99); 51 (p. 65)
9	1270, 1235	-O- (aromatic)	50 (p. 140)
10	1100	C-N	50 (p. 147)
11	1015	-O- (acyclic)	50 (p. 140); 51 (p. 60)
12	920	Phenyl (tri-substituted)	51 (p. 54)
13	845	Phenyl (para- or tri-substituted)	50 (p. 115); 51 (p. 54)
14	775	Phenyl (para- or tri-substituted)	51 (p. 54)
15	740	Imide ring	52 (p. 31)
16	680	Phenyl (mono-substituted)	51 (p. 54)
17	625	$-CH_3$	50 (p. 110)

TABLE IV.- CHANGES IN ABSORPTION BAND MAGNITUDES OF ULTEM DUE TO RADIATION EXPOSURE

Infrared band	Change
C-H (phenyl)	Increase
C-H (methyl)	Decrease
C=O	No change (1.6×10^9 and 4.0×10^9 rad) Decrease (6.0×10^9 rad)
Ether (aromatic)	Decrease
C-N	No change
Tri- and di-substituted phenyl	Decrease
Mono-substituted phenyl	Increase
Imide ring	No change (1.6×10^9 and 4.0×10^9 rad) Decrease (6.0×19^9 rad)

TABLE V.- TENSILE PROPERTIES OF IRRADIATED ULTEM SPECIMENS

Dose, 10^9 rad	Ultimate stress, 10^4 psi	Modulus, 10^5 psi	Elongation to failure, %
1.6	1.58 ± 0.96	4.01 ± 0.49	112 ± 7.1
4.0	1.36 ± 0.08	4.33 ± 0.29	11.5 ± 1.0
6.0	1.49 ± 0.15	4.67 ± 0.57	8.1 ± 1.3
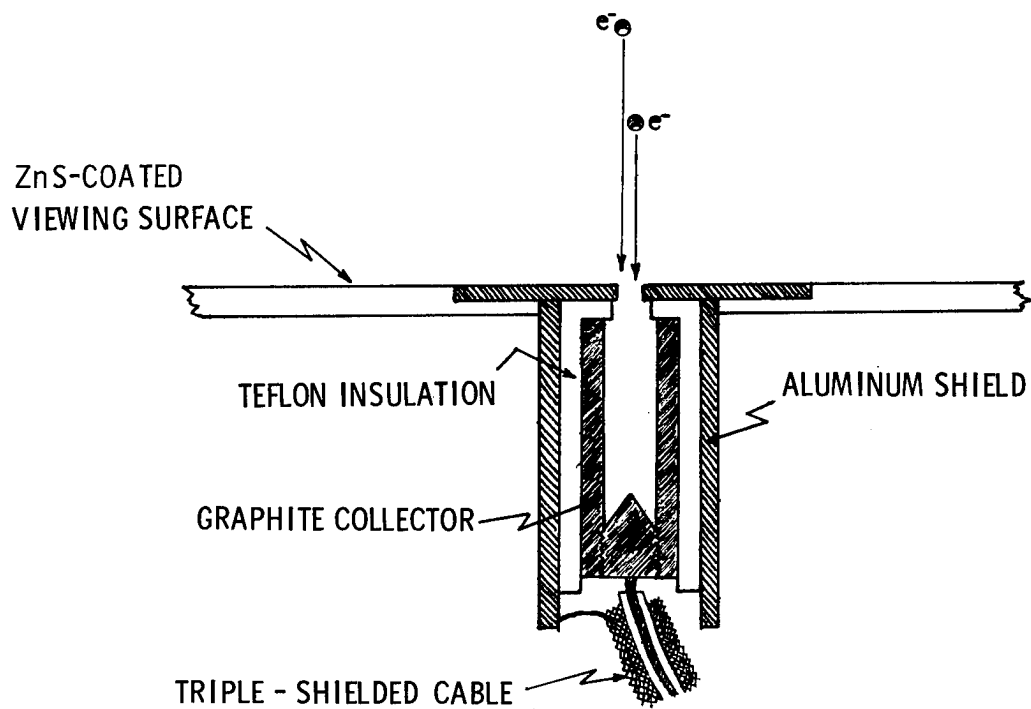
Figure 1.- Cross-sectional drawing of Faraday cup.
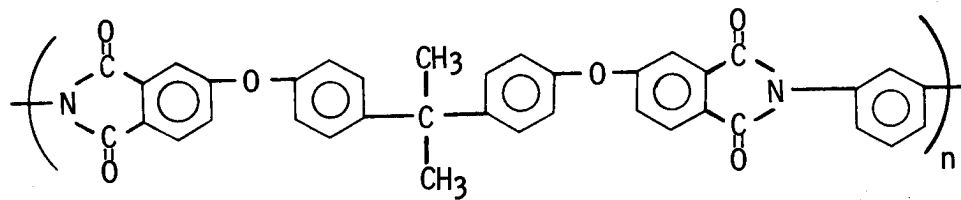
Figure 2.- Molecular structure of nonirradiated Ultem.
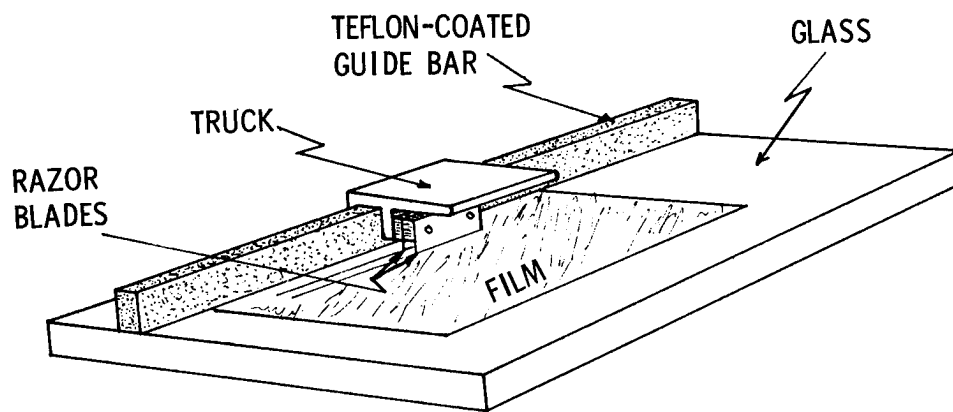
Figure 3.- Fixture for cutting strips from film for mechanical and electron paramagnetic resonance specimens.
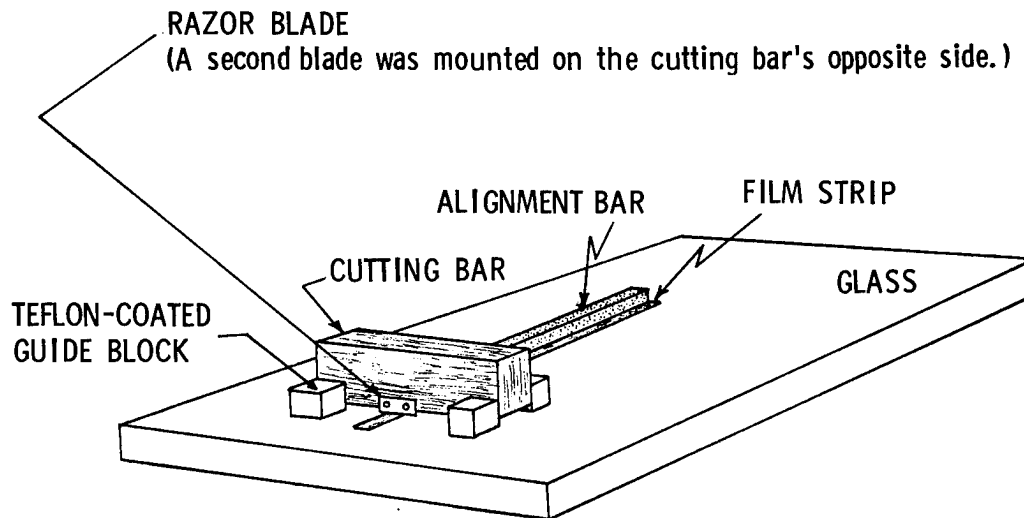
Figure 4.- Fixture for preparing the lengths of the electron paramagnetic resonance specimens.

MECHANICAL SPECIMEN

METAL FRAME
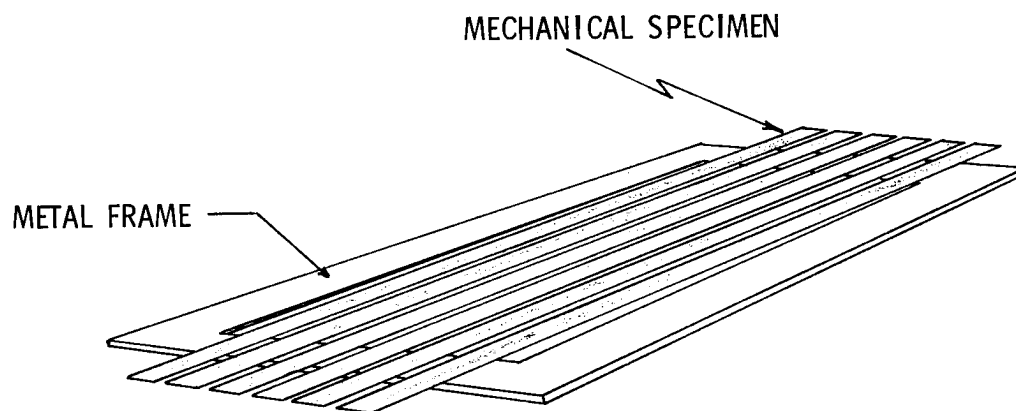
Figure 5.- Configuration of mounting mechanical specimens for
radiation exposure.

ELECTRON PARAMAGNETIC RESONANCE SPECIMEN

WIRE

METAL STRIP
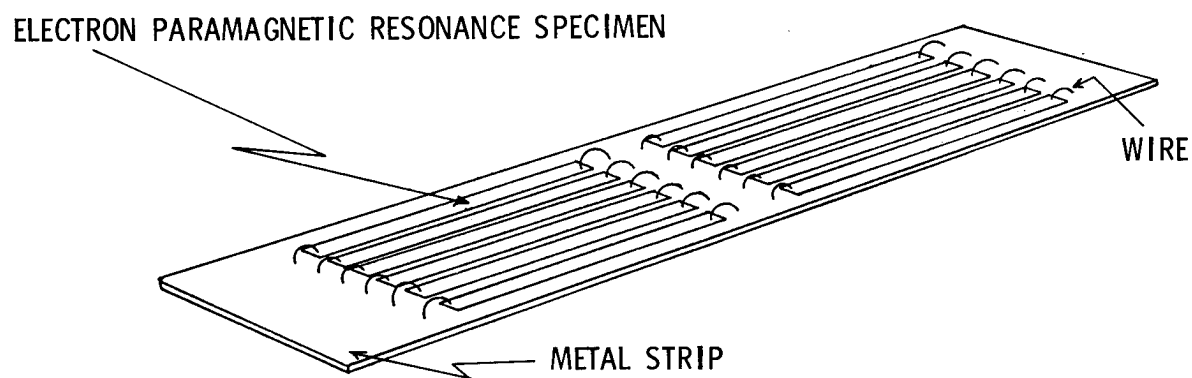
Figure 6.- Configuration of mounting electron paramagnetic resonance
specimens for radiation exposure.
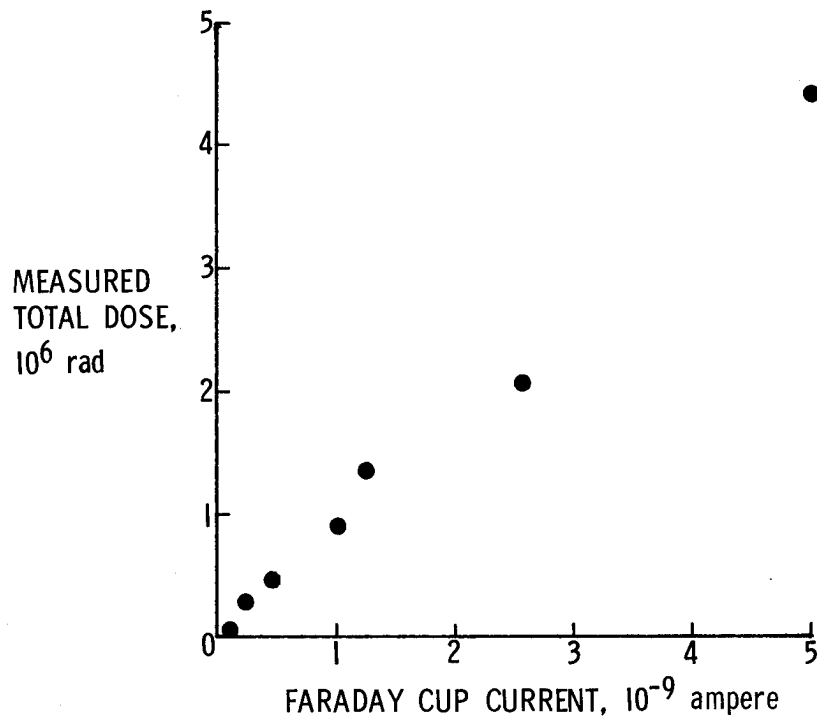
Figure 7.- Relation of Faraday cup current to radiation dose for NBS-standard nylon film, 1-minute exposures.
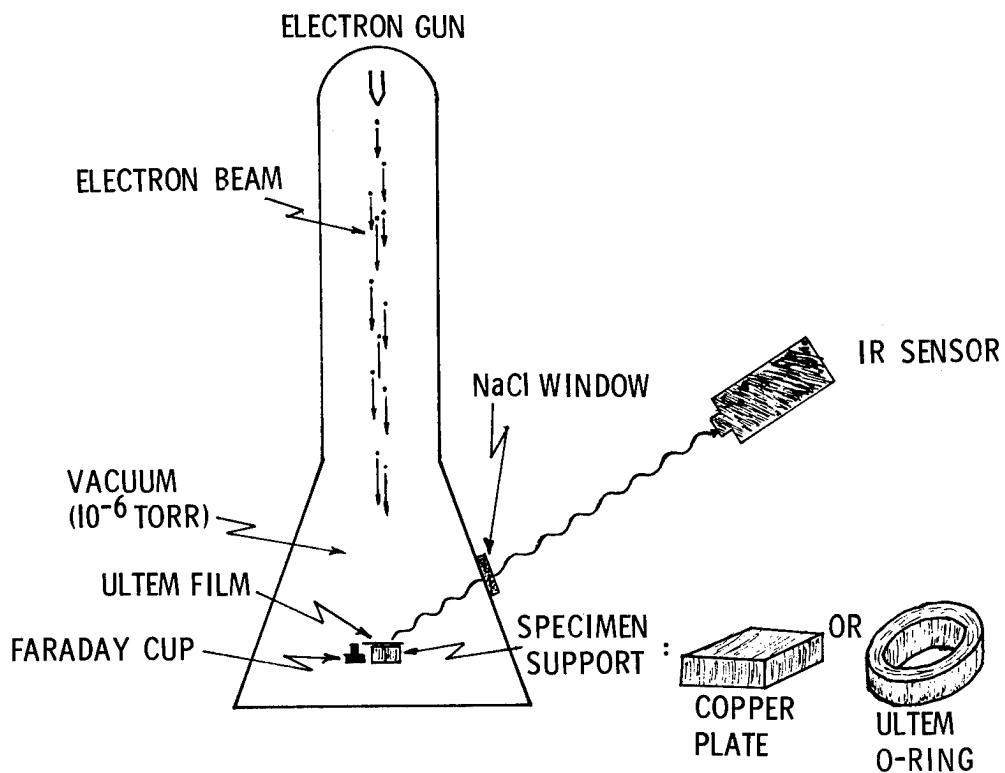
Figure 8.- Configuration for remote infrared monitoring of specimen temperature.
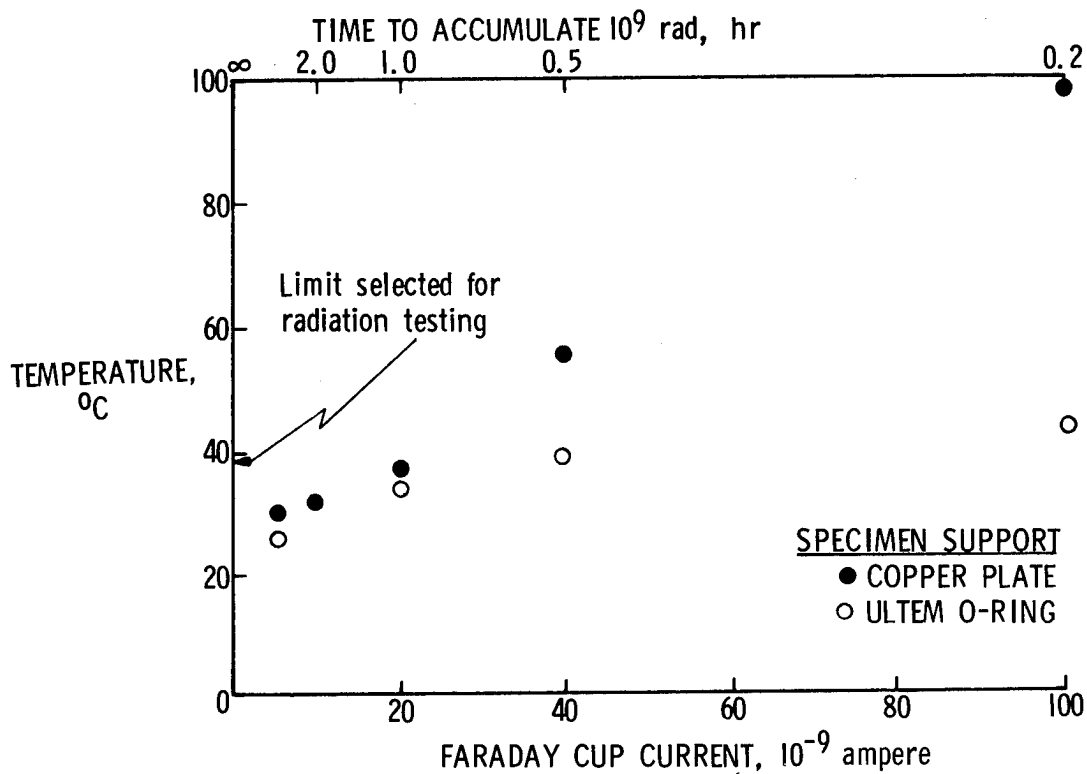
Figure 9.- Specimen temperatures as measured remotely by infrared method for selected dose rates.
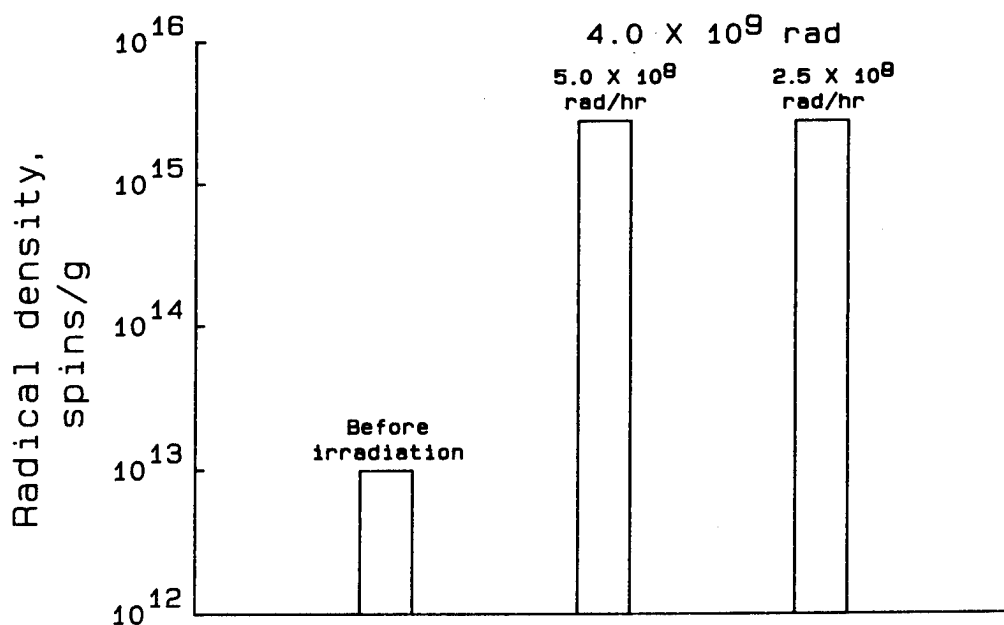
Figure 10.- Spin density values for a dose of 4 × 10^9 rad at dose rates of 5.0 × 10^8 and 2.5 × 10^8 rad/hr.
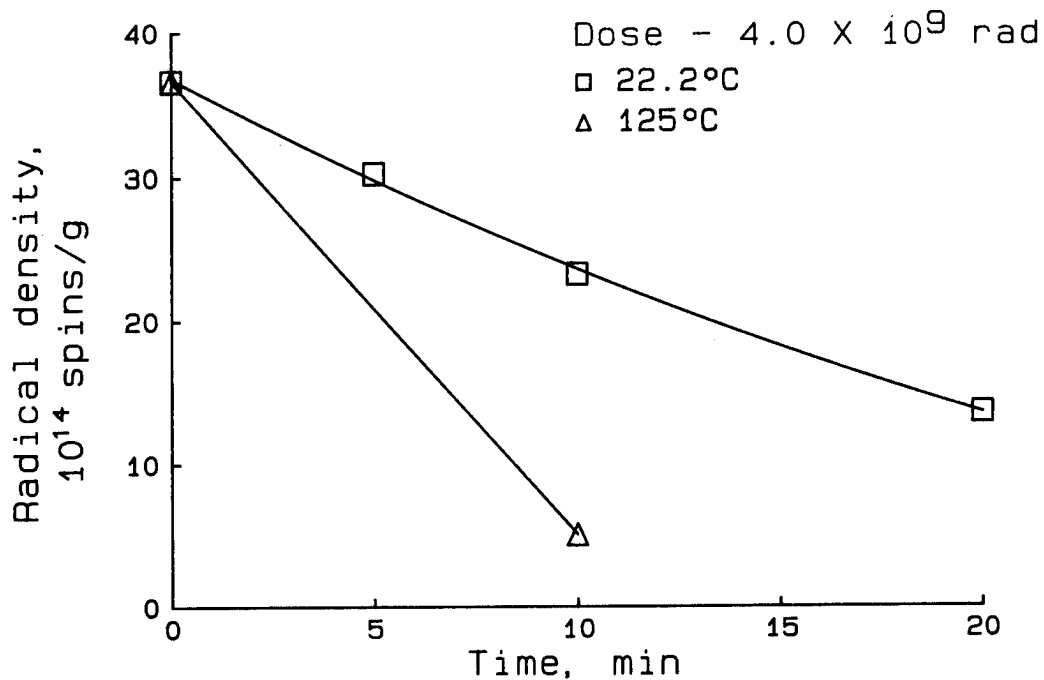
Figure 11.- Radical decay at 22°C and 125°C for irradiated Ultem in air.
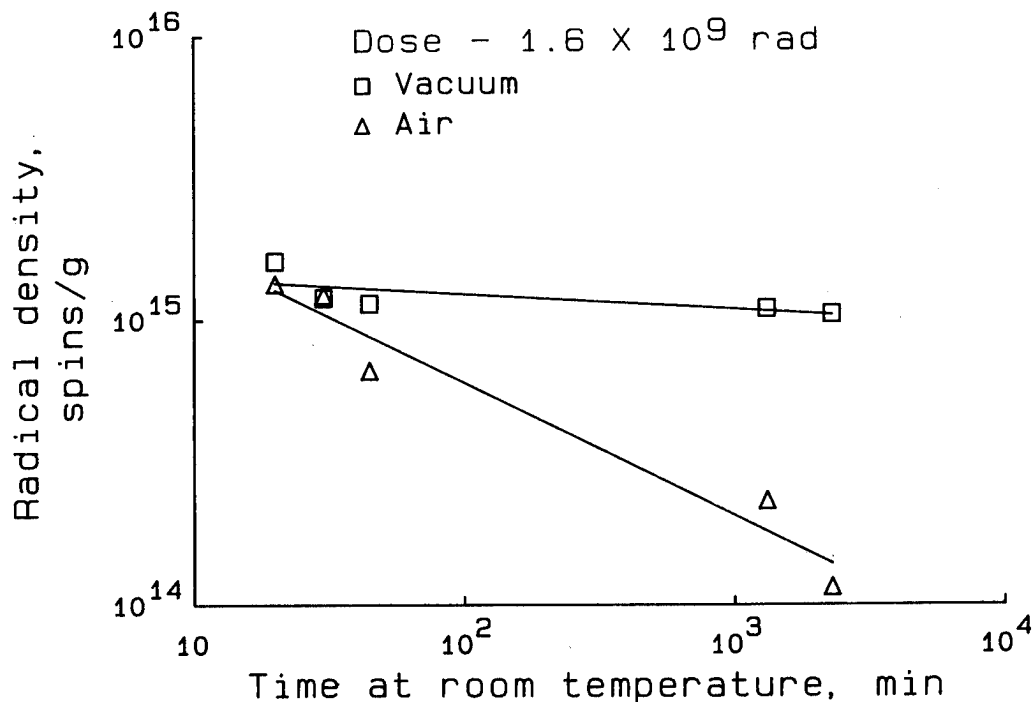
Figure 12.- Radical decay at 22°C in vacuum and in air for irradiated Ultem.

1: Phenoxyls
2: Gem-dimethyls
3: Carbonyls
4: Cyclohexadienyls
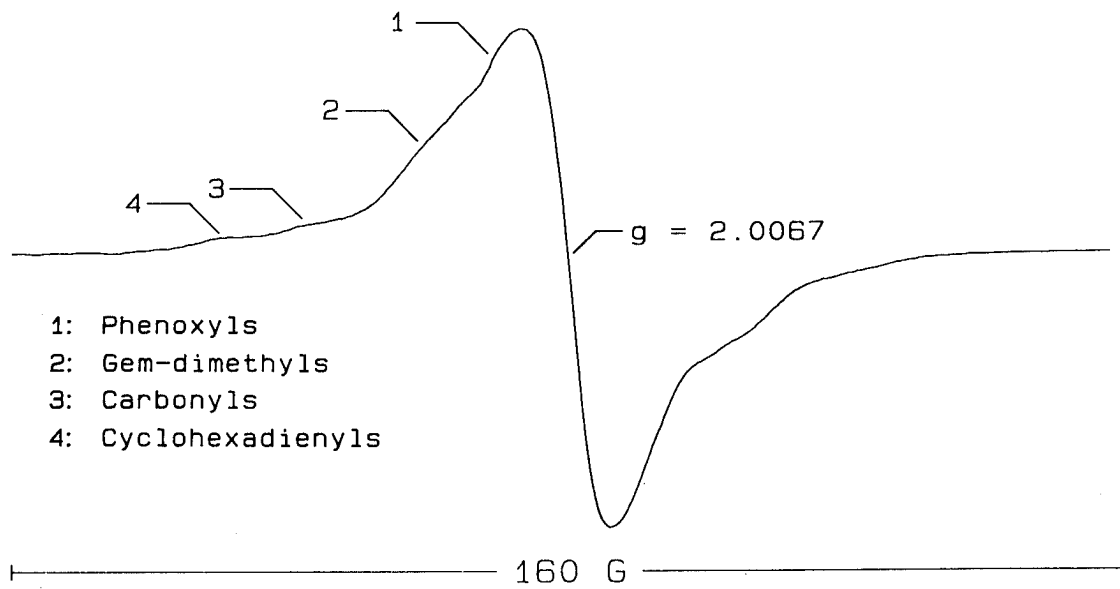
Figure 13.- Identification of radicals in irradiated Ultem, under vacuum.
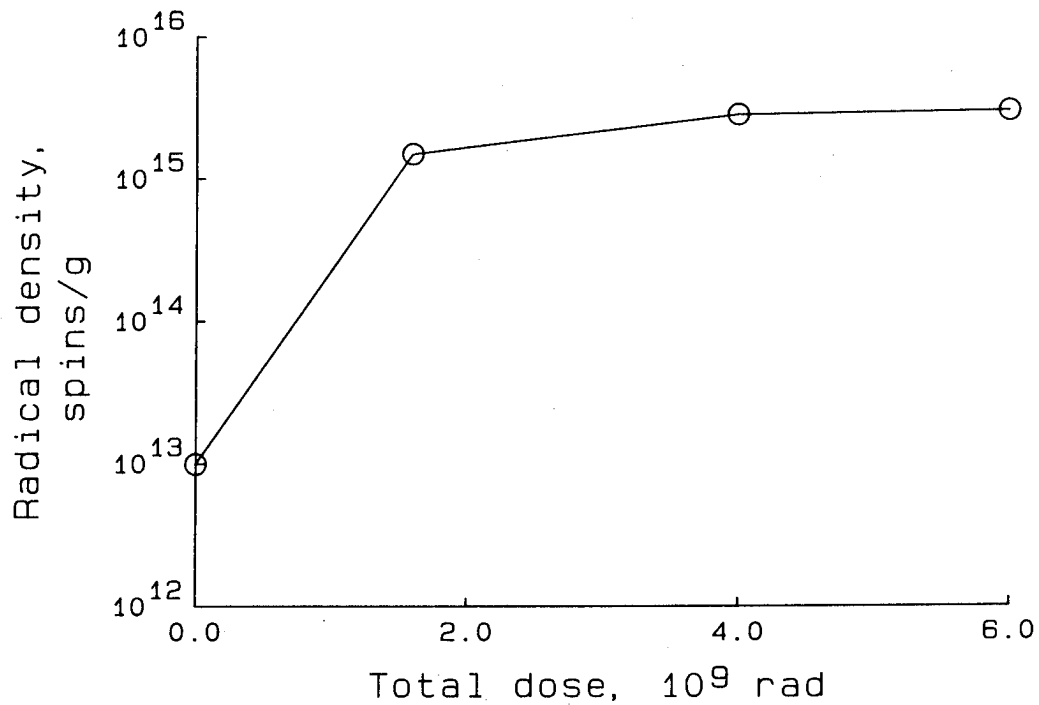
Figure 14.- Radical density for irradiated Ultem as a function of total dose.
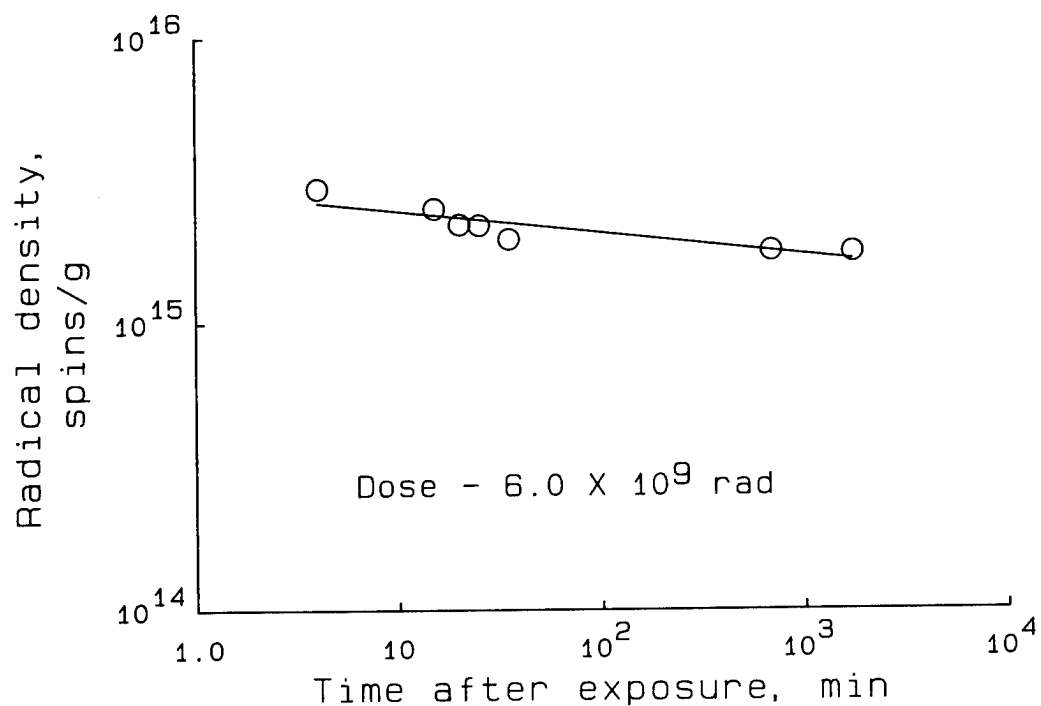
Figure 15.- Radical decay in vacuum as a function of time at 22°C
for irradiated Ultem.
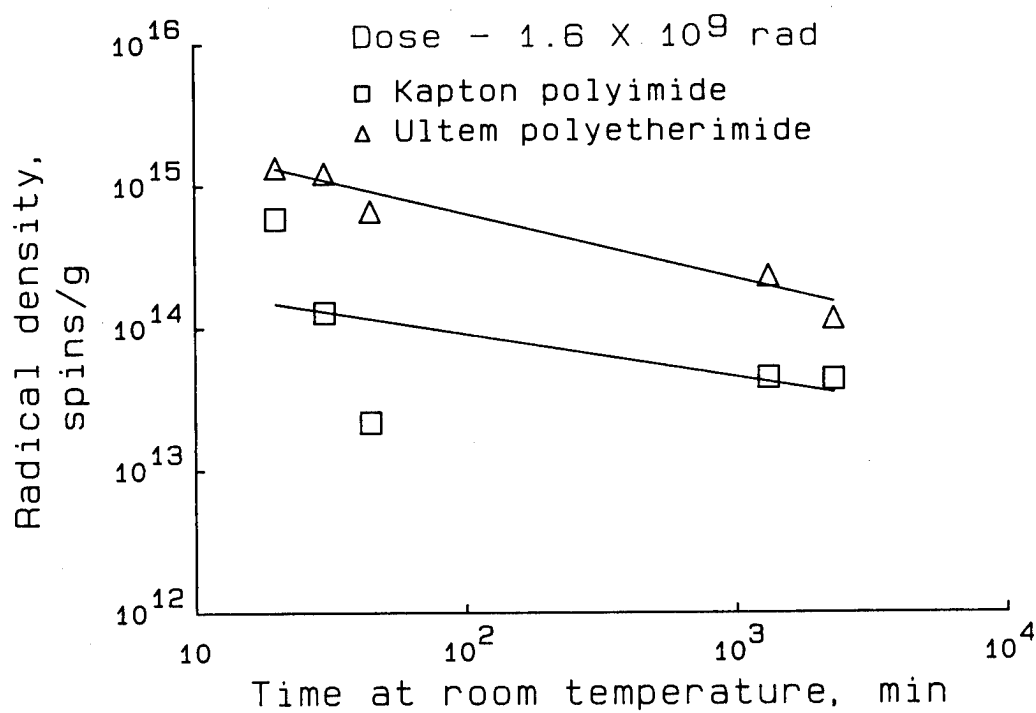
Figure 16.- Radical decay at 22°C in air for irradiated Ultem
and irradiated Kapton.

27
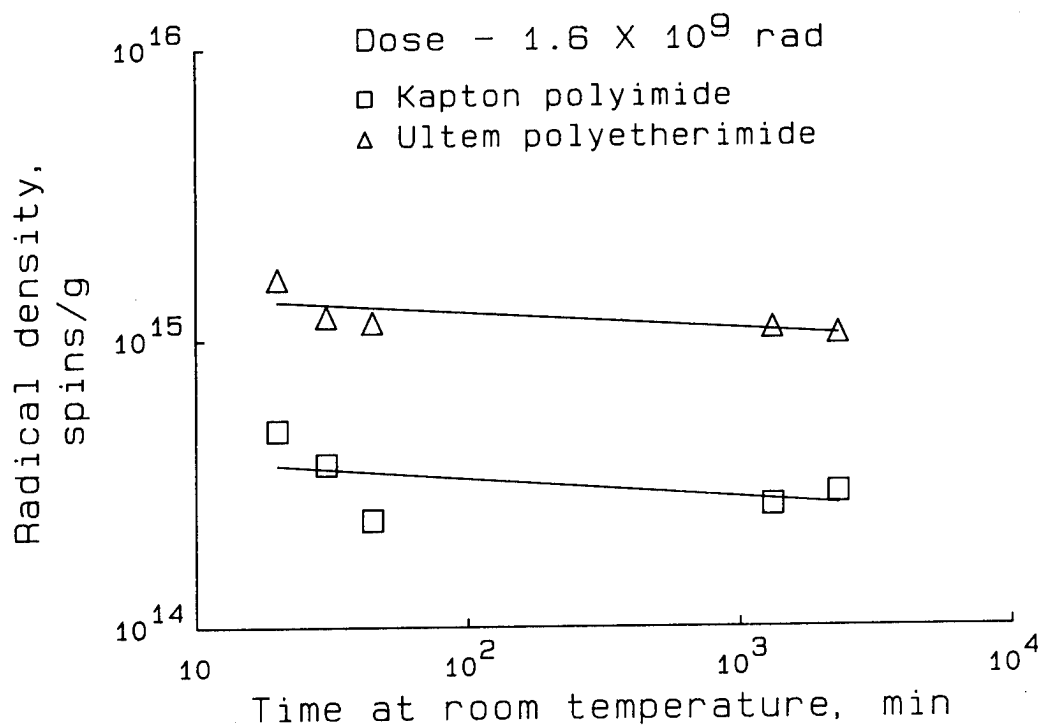
Figure 17.- Radical decay at 22°C in vacuum for irradiated Ultem and irradiated Kapton.
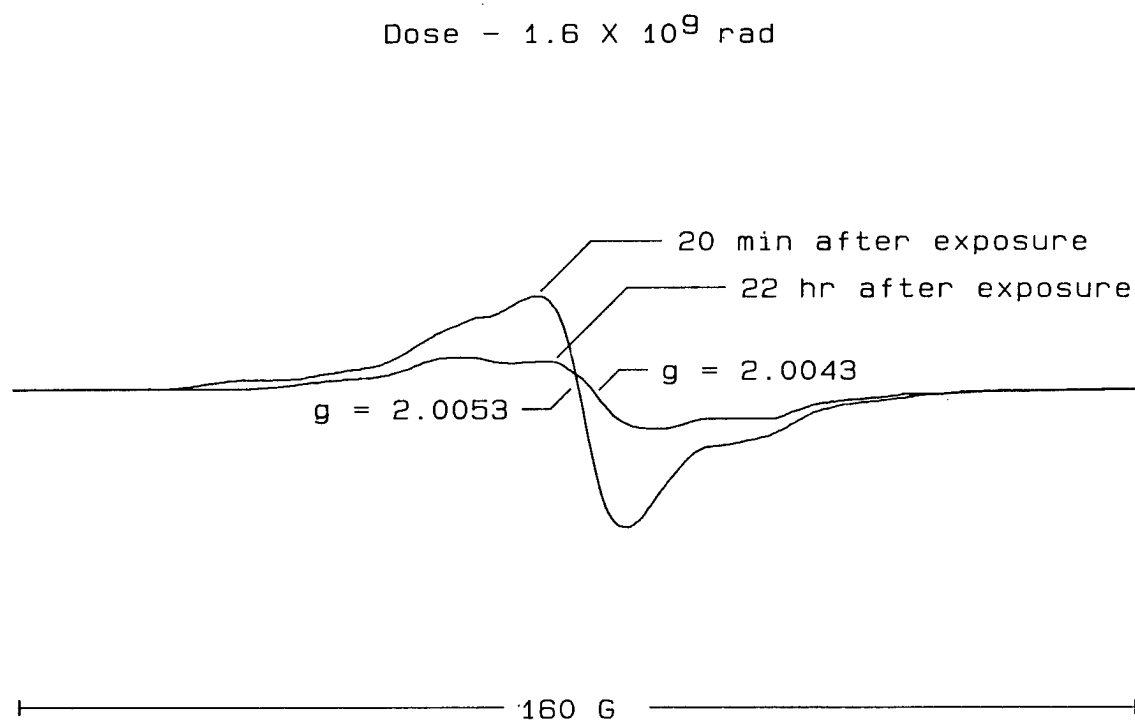
Figure 18.- Relative decay in vacuum at 22°C of radicals in irradiated Ultem, 1.6×10^9 rad dose.

Dose - 6.0 X 10^9 rad

4 min after exposure

28 hr 40 min after exposure

g = 2.0058

g = 2.0067

160 G
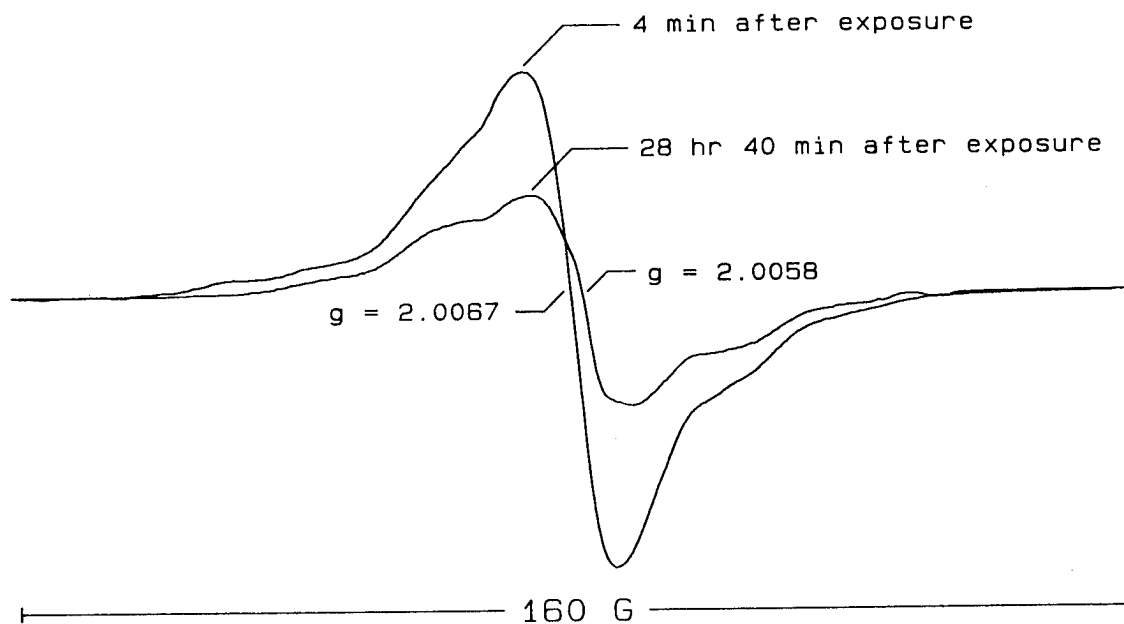
Figure 19.- Relative decay in vacuum at 22°C of radicals in irradiated Ultem, 6.0 × 10^9 rad dose.

Time - less than half hour after exposure

6.0 X 10^9 rad

1.6 X 10^9 rad

g = 2.0053

g = 2.0067

160 G
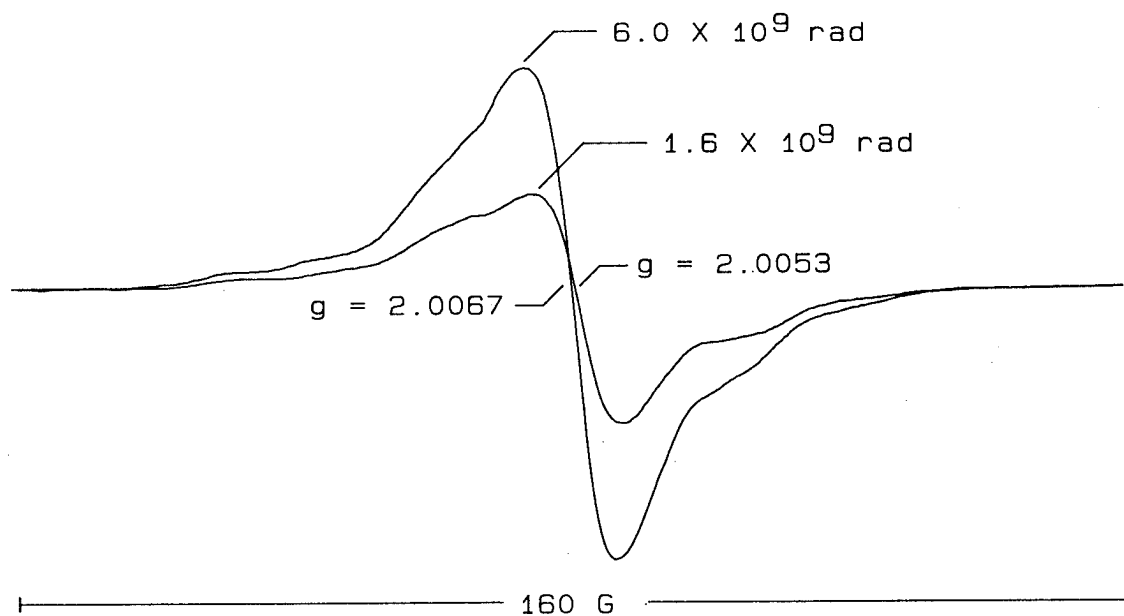
Figure 20.- Comparison for two radiation doses of the radical distribution in Ultem after 20 minutes of decay in vacuum at 22°C.

29

Time — approximately one day after exposure
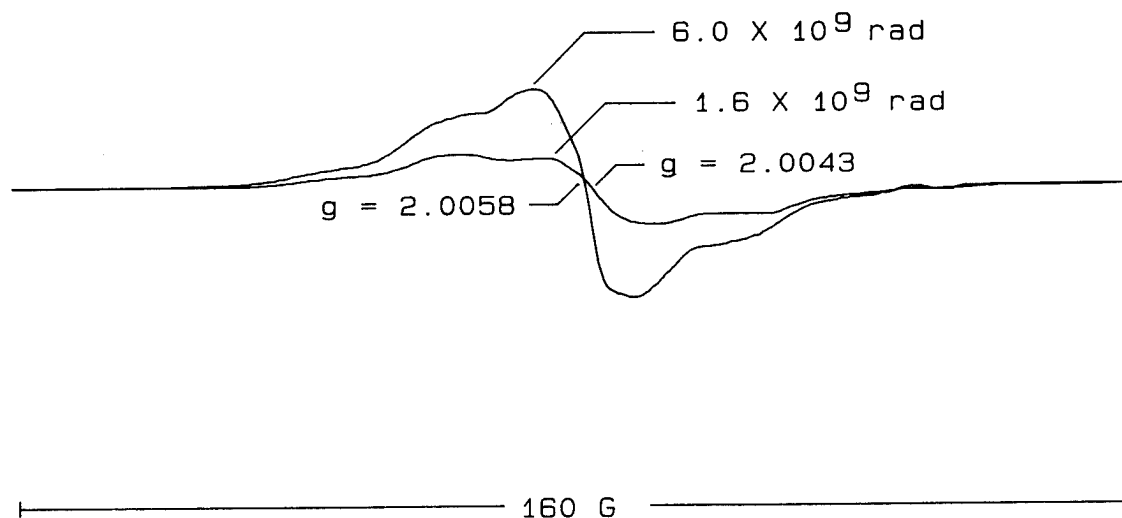
Figure 21.- Comparison for two radiation doses of the radical distribution in Ultem after one day of decay in vacuum at 22°C.
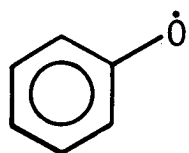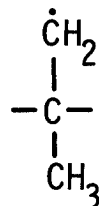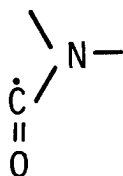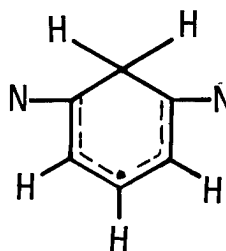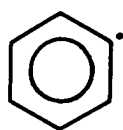
Figure 22.- Identification of structures of radicals in irradiated Ultem, under vacuum.
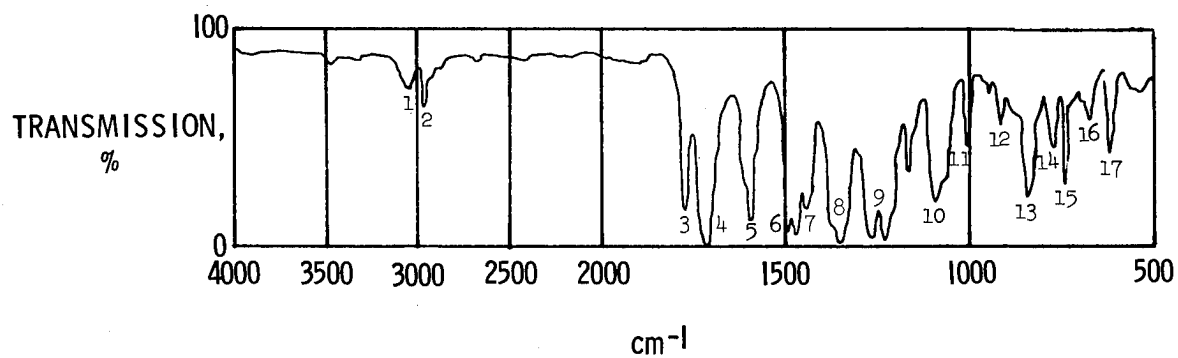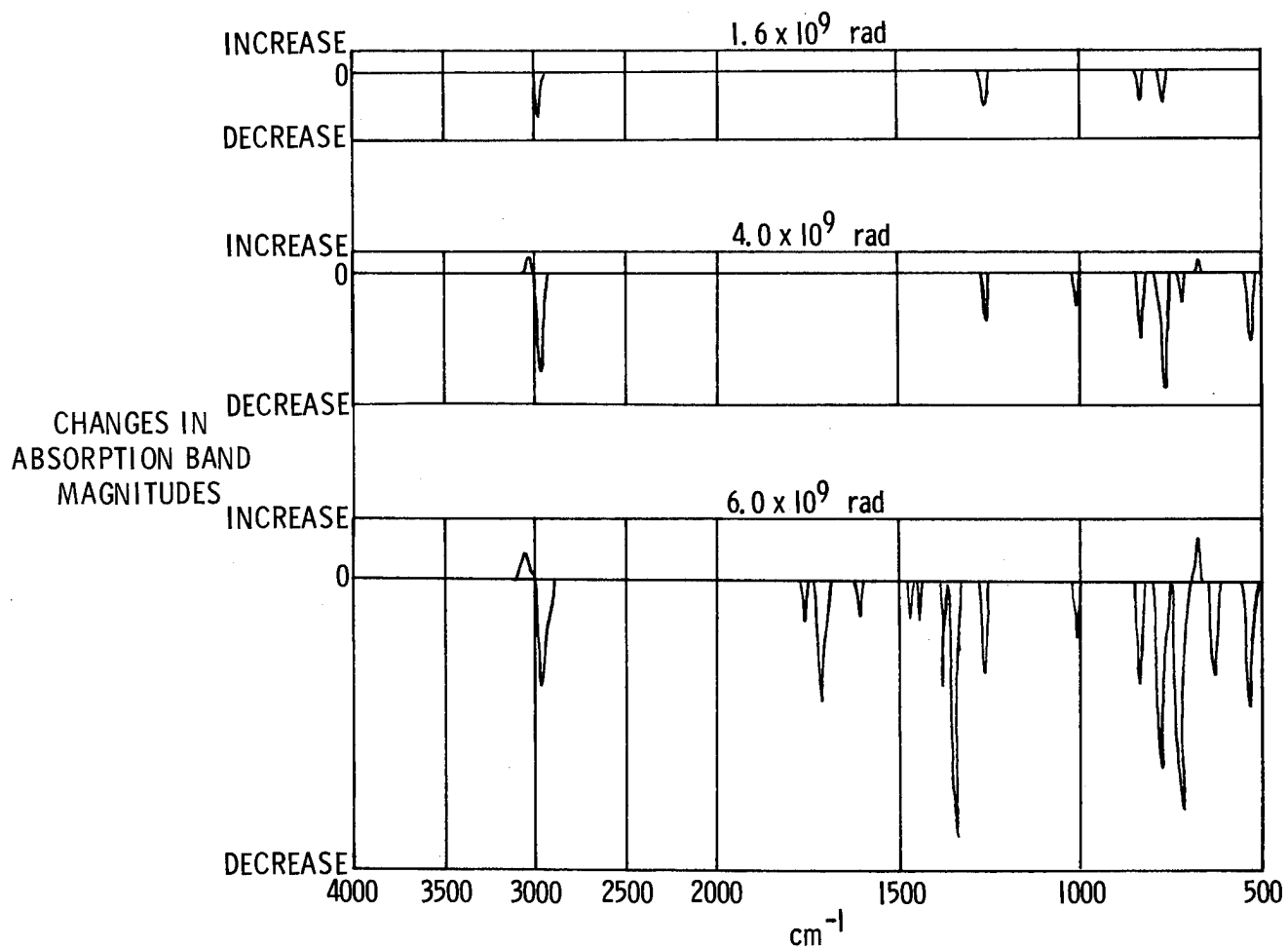
Figure 23.- Infrared spectrum for nonirradiated Ultem.

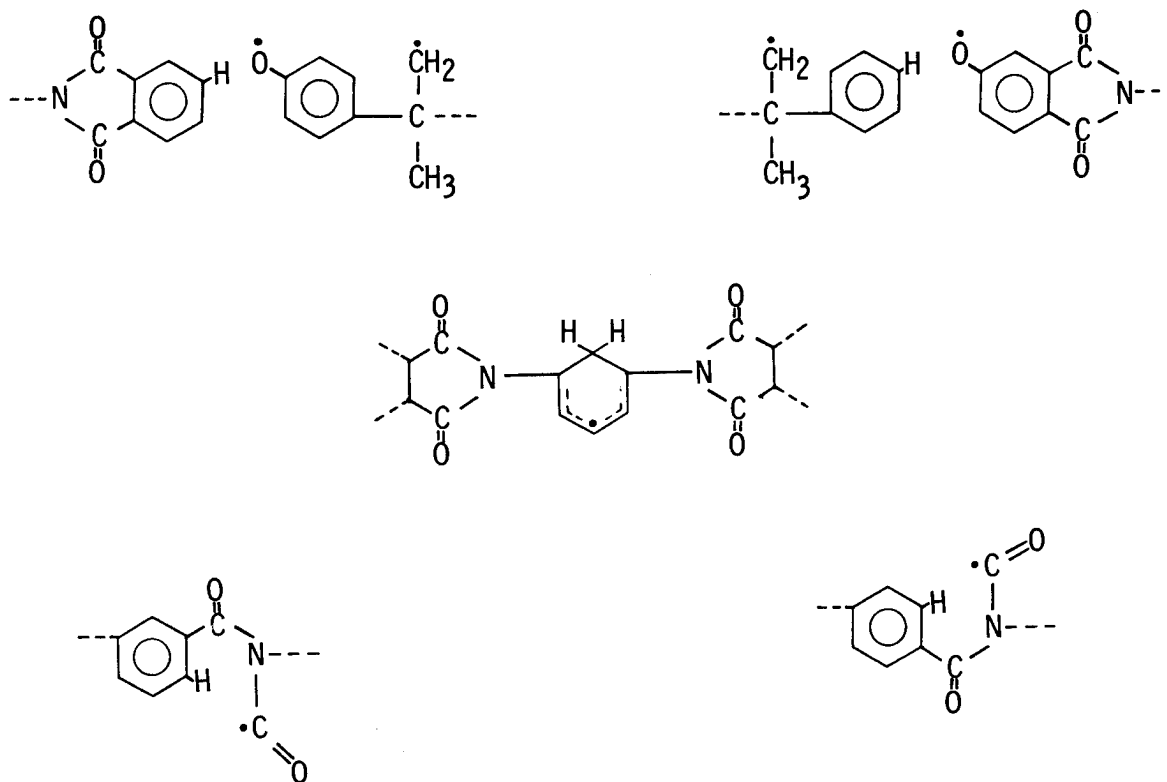Figure 24.- Infrared difference spectra for Ultem before and after irradiation.

Figure 25.- A proposed model for radiation effects on the molecular structure of Ultem, in vacuum.
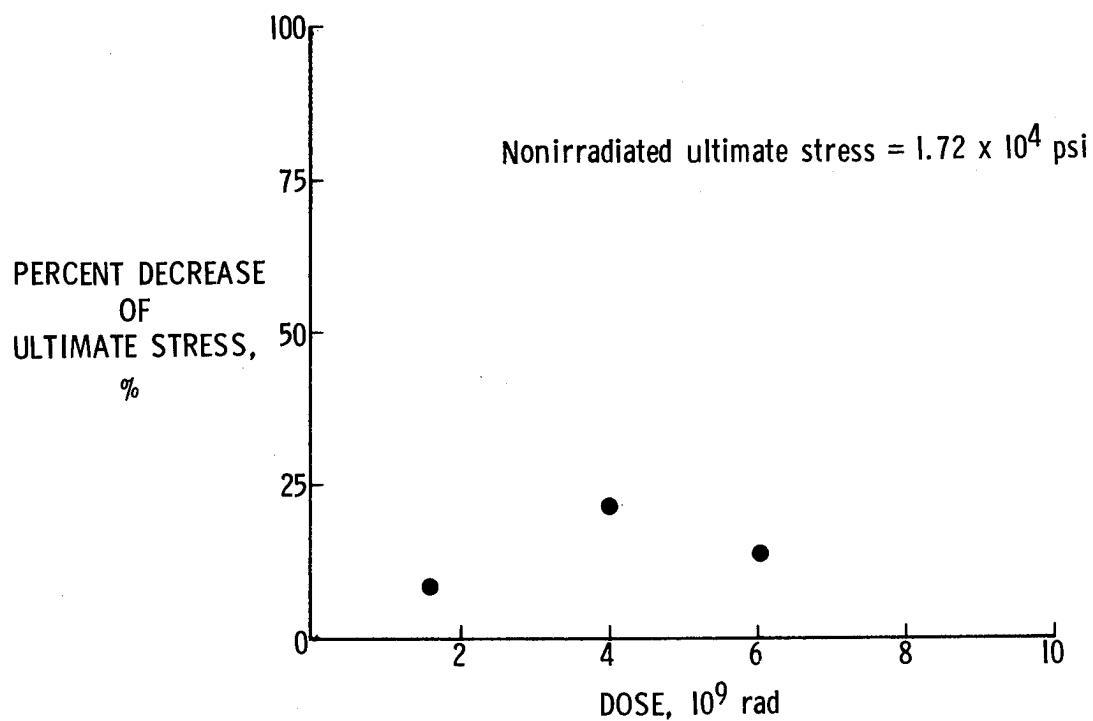

Figure 26.- Change in ultimate tensile stress of Ultem with radiation dose.
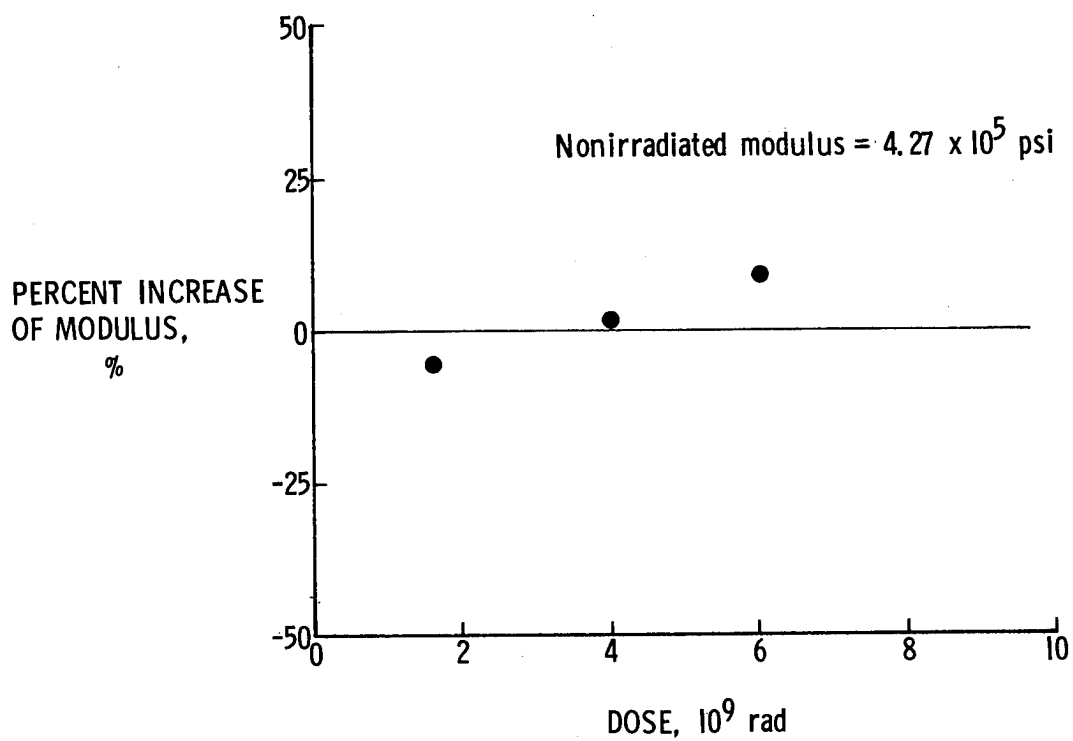
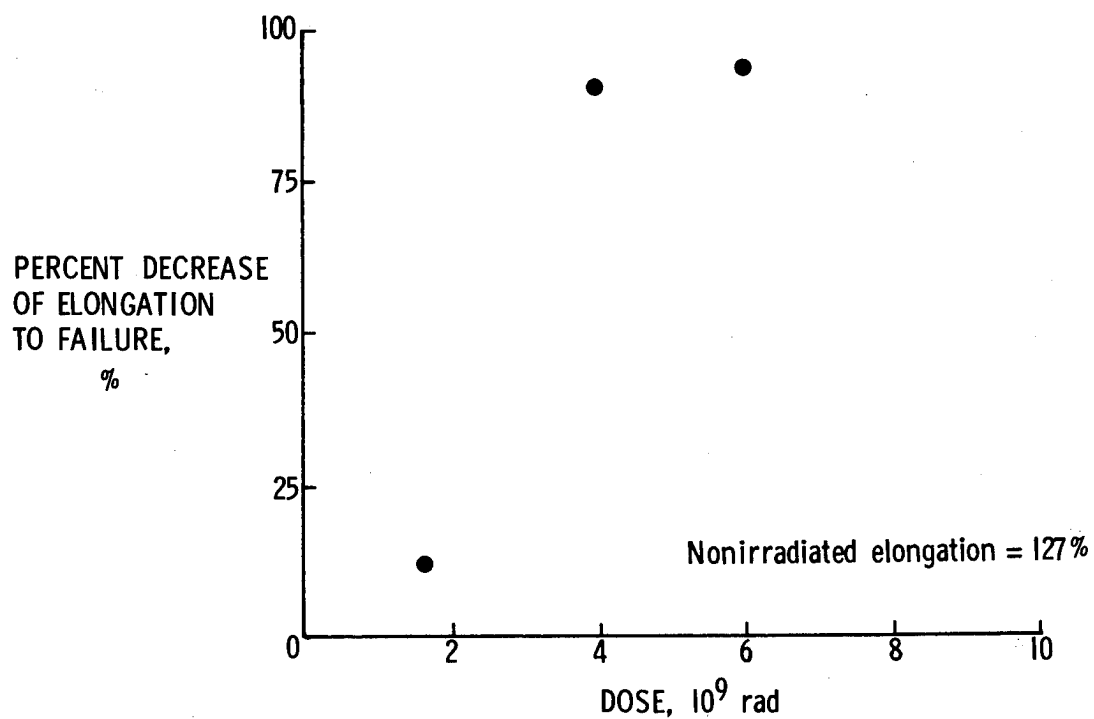Figure 27.- Change in tensile modulus of Ultem with radiation.

Figure 28.- Change in elongation to failure of Ultem with radiation.
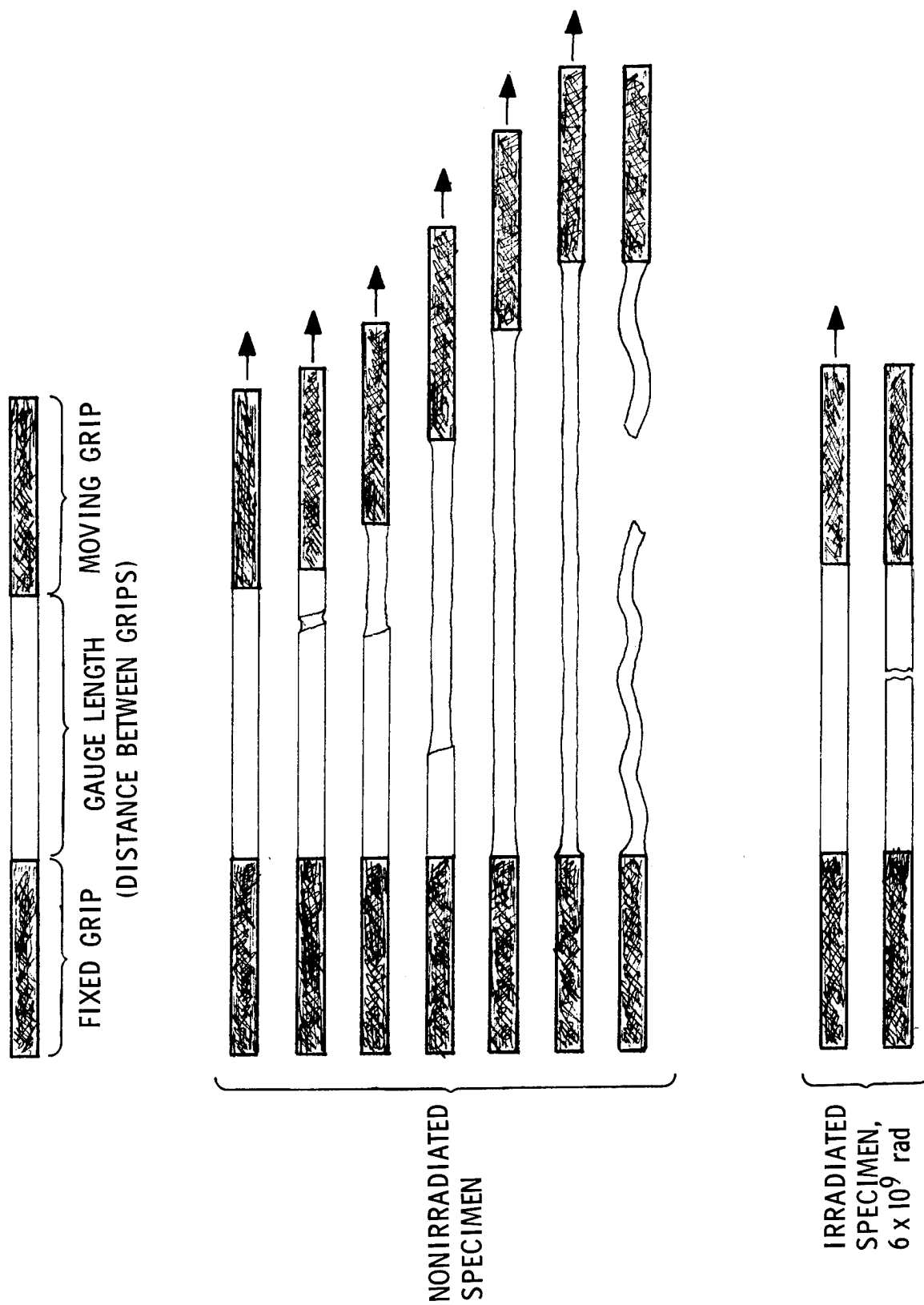
33

FIXED GRIP   GAUGE LENGTH   MOVING GRIP
(DISTANCE BETWEEN GRIPS)

NONIRRADIATED
SPECIMEN

IRRADIATED
SPECIMEN,
6×10^9 rad

Figure 29.— Physical appearance of irradiated and nonirradiated tensile
specimens of Ultem during test.

1. Report No. NASA TP-2429	2. Government Accession No.	3. Recipient's Catalog No.
4. Title and Subtitle Spectroscopic Analysis of Radiation-Generated Changes in Tensile Properties of a Polyetherimide		5. Report Date May 1985
		6. Performing Organization Code 506-53-23-01
7. Author(s) Edward R. Long, Jr., and Sheila Ann T. Long		8. Performing Organization Report No. L-15873
		10. Work Unit No.
9. Performing Organization Name and Address NASA Langley Research Center Hampton, VA 23665		11. Contract or Grant No.
		13. Type of Report and Period Covered Technical Paper
12. Sponsoring Agency Name and Address National Aeronautics and Space Administration Washington, DC 20546		14. Sponsoring Agency Code

15. Supplementary Notes

16. Abstract

The effects of electron radiation on Ultem, a polyetherimide manufactured by General Electric, were studied for doses from 2×10^9 to 6×10^9 rad. Specimens for tensile property testing and for electron paramagnetic resonance and infrared spectroscopic measurements of molecular structure were studied. Miniature tensile specimens, for which the size and testing procedures were developed, were used because the size of the exposure area was limited. Also, a new Faraday cup design and a method for remote temperature measurement were developed. The spectroscopic data showed that radiation caused dehydrogenation of methyl groups, rupture of main-chain ether linkage, and opening of imide rings, all to form radicals. The spectroscopic data also indicated that the so-formed atomic hydrogen attached to phenyl radicals, but not to phenoxyl radicals, which would have formed hydroxyls. Therefore, the observed decays of the radiation-generated phenoxyl, gem-dimethyl, and carbonyl radicals were interpreted as a combining of the radicals to form crosslinking. This crosslinking is the probable cause of the major reduction in the elongation of the tensile specimens after irradiation. Subsequent classical solubility tests indicated that the irradiation did cause massive crosslinking.

17. Key Words (Suggested by Author(s)) Radiation effect Space radiation Polyimide Spectroscopy Tensile property Infrared Large space structures Electron paramagnetic resonance		18. Distribution Statement Unclassified - Unlimited Subject Category 24
19. Security Classif. (of this report) Unclassified	20. Security Classif. (of this page) Unclassified	21. No. of Pages 36 22. Price A03